TcdE: the silent member in the pathogenicity locus of *Clostridium difficile*?

Der Naturwissenschaftlichen Fakultät der
Gottfried Wilhelm Leibniz Universität Hannover
zur Erlangung des Grades
Doktorin der Naturwissenschaften
Dr. rer. nat.
genehmigte Dissertation von

Dipl. Biochem. Alexandra Olling
geboren am 02.10.1980 in Barßel

- 2009 -

Die vorliegende Arbeit wurde in der Zeit von Juli 2006 bis Juni 2009 im Institut für Toxikologie der Medizinischen Hochschule Hannover unter der Betreuung von PD Dr. Ralf Gerhard angefertigt.

Referent: PD Dr. Ralf Gerhard

Korreferent: Prof. Dr. Mathias Walter Hornef

Tag der Promotion: 14. August 2009

Eidesstattliche Erklärung

Hiermit versichere ich an Eides statt, die vorliegende Dissertation selbstständig verfasst und die benutzten Hilfsmittel sowie Quellen vollständig angegeben zu haben.

Ich habe die Dissertation nicht als Diplomarbeit oder ähnliche Arbeit verwendet und abgesehen von den angegebenen Teilpublikationen nicht veröffentlicht.

Hannover, den 04. Juni 2009

_____

(Unterschrift)

Danksagung

Zunächst danke ich PD Dr. Ralf Gerhard für die ausgezeichnete Betreuung während meiner Dissertation. Auf seine Kompetenz, aber auch seine Gelassenheit, konnte man stets vertrauen.

Ein herzlicher Dank geht an Prof. Dr. Ingo Just für hilfreiche Diskussionen und nützliche Denkanstöße.

Weiterhin bedanke ich mich bei Prof. Dr. Mathias Hornef für die Übernahme des Korreferates.

Ich danke allen Mitarbeitern des Institutes für ihre Kollegialität und viele private Stunden. Bei Helma Tatge bedanke ich mich überdies für ihre Fürsorge und tatkräftige Unterstützung.

Ein ganz besonderer Dank gilt meiner Familie und meinem Freund Mirco Müller, auf deren Unterstützung ich uneingeschränkt bauen konnte. Ich weiß Euer Vertrauen in mich und meine Entscheidungen sehr zu schätzen.

Abstract

Clostridium difficile is the causative agent of antibiotic-associated diarrhea and pseudomembranous colitis and the most important reason of nosocomial infections. The major virulence factors are toxins A and B, which are encoded by the pathogenicity locus (PaLoc). The small open reading frame *tcdE* within the PaLoc is located between the genes for the pathogenic toxins A (TcdA) and B (TcdB). The role of the deduced 19 kDa protein TcdE with respect to *C. difficile* virulence is not yet known. Sequence and structure homologies to bacteriophage encoded holins led to the hypothesisof a TcdE-induced release of the pathogenic toxins from *C. difficile* into the extracellular environment as consequence of bacterial lysis. Further assumptions focused on a *tcdE*-mediated regulation of the toxin genes, however, both hypotheses lack evidences so far.

The present study investigates a potential impact of TcdE on *Escherichia coli* K12 as representatives of the commensals residing in the *C. difficile* habitat. TcdE function was further analyzed with respect to *C. difficile* growth, sporogenesis and toxin release by generating a TcdE-deficient *C. difficile* mutant strain.

Expression of TcdE in *E. coli* correlated with bacterial cell death monitored by a decrease in cell count accompanied by release of ATP. Structure-function analysis using deletion mutants of TcdE revealed an essential role of the three transmembrane domains with regard to bacteriolysis and a modulatory impact of the N- and C-termini. *TcdE* exhibits an alternative ribosome binding site combined with a dual start motif leading to expression of the 19 kDa full length TcdE and an N-terminal shortened 16 kDa product with a ratio 1 : 10. The truncated TcdE was shown to be crucial for bacteriolysis and the full length form to inhibit lysis function.

Since full length as well as truncated TcdE did not damage isolated mitochondria, affect cell and nuclei morphology or induce apoptotic cascades after transfection in epithelial cells, TcdE is unlikely to be a pathogenicity factor acting on target cells of *C. difficile*.

Analyses of the TcdE-deficient *C. difficile* mutant revealed that TcdE does not regulate *C. difficile* growth or sporogenesis. Furthermore, TcdE knockout neither alters kinetic of toxin release nor the absolute TcdA and TcdB protein levels, refuting the often discussed hypothesis of a TcdE-mediated release of the pathogenic toxins as a result of bacterial lysis. The present study disproves TcdE to function as virulence factor or the controversially discussed cause for toxin release. However, TcdE was shown to induce cell death of Gram negative bacteria by an N-terminal truncated form which is not produced in *C. difficile*. Data indicate that TcdE might have antimicrobial impact on intestinal commensals or prevent the virulence mediating pathogenicity locus of *C. difficile* from being utilized by other bacterial species since expression of short TcdE would cause cell death.

Key words: *Clostridium difficile*, TcdE, bacterial lysis

Zusammenfassung

Clostridium difficile ist der Auslöser der Antibiotika- assoziierten Diarrhöe und Pseudomembranösen Colitis und stellt den Hauptversursacher nosokomialer Infektionen dar. Der kleine offene Leserahmen *tcdE* innerhalb des *C. difficile* Pathogenitätslocus' ist zwischen den Genen der pathogenen Toxine A (TcdA) und B (TcdB) lokalisiert. Bisher ist unklar, welche Rolle das putative 19 kDa- Protein TcdE bei der Virulenz von *C. difficile* spielt. Sequenz- und Strukturhomologien zwischen TcdE und Bakteriophagen-codierten Holinen führten zur Hypothese einer Freisetzung von TcdA/B infolge einer TcdE-verursachten Bakteriolyse. Alternativ wurde eine *tcdE*-vermittelte Regulation der Toxin-Gene vermutet. Für beide Hypothesen wurden bislang keine eindeutigen Beweise erbracht.

Die vorliegende Arbeit untersucht die Wirkung von *C. difficile* TcdE auf *Escherichia coli* K12 als Vertreter intestinaler Kommensalen. Um zusätzlich einen möglichen Einfluss von TcdE auf das Clostridien-Wachstum, die Sporulation oder dessen Toxin-Freisetzung zu analysieren, wurde eine TcdE-defiziente *C. difficile*-Mutante generiert.
Die Expression von TcdE in *E. coli* korrelierte mit einer Bakteriolyse, die durch Reduktion der Bakterienzahl und gleichzeitiger ATP-Freisetzung erfasst wurde. Struktur- Wirkungs-Analysen mit TcdE- Deletionsmutanten konnten eine essentielle Rolle der drei Transmembran-domänen und eine Modulatorfunktion des N- und C- Terminus' deutlich machen. Eine alternative Ribosomen-Bindestelle kombiniert mit einem dualen Startmotiv innerhalb der *tcdE*- mRNA führten zur Expression des Holo-TcdEs (19 kDa) und einer N- terminal verkürzten Form (16 kDa). Die Studie belegt, dass die Bakteriolyse durch das verkürzte TcdE vermittelt wird, wohingegen das Holo-TcdE als dessen Antagonist, dem Lyse-Inhibitor, agiert. Eine potentielle Funktion von TcdE als weiterer Pathogenitätsfaktor wurde durch Transfektionsexperimente untersucht. Da weder das Holo-TcdE noch die verkürzte Form die Zell- oder Zellkern-Morphologie beeinflussen, zu einer Schädigung isolierter Mitochondrien führen oder Apoptose induzieren, wird eine pathogene Wirkung von TcdE ausgeschlossen.
Zur weiteren Untersuchung der Funktion von TcdE wurde über die ClosTron-Technik das *tcdE*-Gen in Clostridien funktionell inaktiviert. Mithilfe dieser TcdE-defizienten *C. difficile*-Mutante konnte gezeigt werden, dass TcdE weder in die Regulation des *C. difficile*-Wachstums oder der Sporulation involviert ist, noch die oft diskutierte Freisetzung der Toxine A und B als Folge von Bakteriolyse bewirkt.
Die Ergebnisse der vorliegenden Arbeit schließen eine Funktion von TcdE als Virulenzfaktor aus und widerlegen die kontrovers diskutierte Hypothese einer TcdE- vermittelten Freisetzung der Pathogenitätsfaktoren. Allerdings induziert TcdE über eine N- terminal verkürzte Form die Lyse Gram-negativer Bakterien, was auf eine potentielle antimikrobielle Wirkung gegenüber intestinalen Kommensalen hindeutet. Alternativ könnte TcdE vor einer „Fremdnutzung" des PaLoc schützen, da dessen Integration in die DNA Gram-negativer Bakterien nach Expression des kurzen TcdE die Lyse der Bakterien zur Folge hätte.

Schlagwörter: *Clostridium difficile*, TcdE, Bakteriolyse

List of contents

1. Introduction

1.1 *Clostridium difficile*

Clostridium difficile is a Gram positive, facultative anaerobic rod of the Clostridiaceae family. The spore-forming bacterium is ubiquitous distributed and resides in the human intestine in 2-5% of the population. *C. difficile* was first described in 1935 when it was found in the intestine of healthy new born infants (Hall and O'Toole, 1935). With the introduction of broad-spectrum antibiotics, antibiotic-associated diseases occurred. Few years later, *C. difficile* was identified as the responsible pathogen causing antibiotic-associated diarrhea and the more severe form, the pseudomambranous colitis (Larrson and Proce, 1977; Bartlett *et al.*, 1978).

In the last centuries, incidence of *C. difficile* associated diseases (CDAD) increased resulting from enhanced application of broad-spectrum antibiotics, such as aminopenicillins, cephalosporins and clindamycin. These antibiotics cause disruption of the normal intestinal flora facilitating colonization and overgrowth of *C. difficile* (Just *et al.*, 2000). *C. difficile* is spread fecal-orally through resistant endospores. Sporulation is of ecological advantage to the organism as it enables to survive under adverse conditions. Thus, sporulation normally occurs under condition of nutrients depletion. A variety of factors such as pH, media composition and ionic strength are known to affect sporulation.

Upon spore ingestion, germination to vegetative cells occurs within the colon followed by proliferation and release of the major pathogenicity factors, toxin A (TcdA) and B (TcdB) (Lyerly and Wilkins, 1995). The toxins are single chain proteins belonging to the family of large clostridial cytotoxins. They share 63 % sequence homology and are responsible for disease manifestations to the greatest extend (Von Eichel-Streiber *et al.*, 1992).

Historically, TcdA (308 kDa) was termed enterotoxin because of inducing typical symptoms of colitis in animal models (Lyerly *et al.*, 1985; Triadafilopoulos *et al.,* 1987). In contrast, TcdB (270 kDa) did not exhibit enterotoxic properties towards animals, but possess a 100- to 1000 higher cytotoxic potency in cell culture than TcdA and thus, was designated as cytotoxin (Lyerly *et al.*, 1982). However, recently it was shown that TcdB is essential for virulence of *C. difficile* since TcdA- deficient *C. difficile* mutants still producing TcdB retained a wildtype virulence phenotype whereas the disruption of exclusively *tcdB* resulted in a significant attenuation of virulence in hamsters (Lyras *et al.*, 2009). *In vitro*, both toxins cause reorganization of the actin cytoskeleton accompanied by shrinking and rounding of the cultured cells (cytopathic effect). This effect is based on a glucosyltransferase activity of TcdA and TcdB towards their substrate proteins, the Rho family GTPases (Just *et al.*, 1995). Both toxins monoglucosylate a Threonin residue within the effector domain of Rho proteins (RhoA

at Thr-37; Rac-1, Cdc42 and Ras at the homolog residue Thr-35) resulting in inhibition of effector coupling and subsequent blocking of signal transduction pathways. Since Rho GTPases regulate dynamics of the actin cytoskeleton (Hall, 1998) toxin-catalyzed glucosylation also affects cell division, migration, morphogenesis (Jaffe and Hall, 2005) and epithelial barrier functions (Riegler *et al.*, 1997; Lawrence *et al.*, 1997; Nusrat *et al.*, 2001; Schoentaube *et al.*, 2009). Furthermore, Rho-GTPases induce apoptosis in cells, designated as cytotoxic effect (Nottrott *et al.*, 2007; Gerhard *et al.*, 2008).

Clinical disease associated with *C. difficile* has varying clinical features ranging from self-limited watery diarrhea with fever, abdominal pain and leycocytosis, to life-threatening pseudomembranous colitis and toxic megacolon (Rubin *et al.*, 1995). The different types of clinical characteristics likely present the result of cellular and molecular interactions between the *C. difficile* toxins and host intestinal defense mechanisms. The toxins trigger the attraction and adhesion of neutrophils resulting in inflammation of the mucosal lining and cellular necrosis, as well as increased capillary permeability due to an opening of the tight junctions, leading to diarrhea and colitis (Poxton *et al.*, 2001; Durai, 2007). In addition, TcdA induces the production of TNF-α and pro-inflammatory interleukins which further facilitate the associated inflammatory response and pseudomembrane formation (Poxton *et al.*, 2001). The pseudomembranes appear as yellow-white plaques composed of neutrophils, fibrin, mucin and cellular debris.

Fig. 1.1: Pseudomembranous colitis. Colonoscopial view of the typical yellow-white pseudomembranous fibrin plaques. Source: www.endoline.de/html/darmerkrankungen.html, 10.05.2009

Diagnosis of infection with pathogenic *C. difficile* typically occurs by detection of the toxins TcdA and TcdB in stool samples by means of enzyme immunoassays (EIA) or the conventional cell cytotoxicity assay (Bartlett and Gerding, 2008).

C. difficile associated disease (CDAD) is usually treated orally with metronidazole or vancomycin following cessation of the inciting antibiotics. Metronidazole and vancomycin are comparable regarding efficacy and relapse rates (Wenisch *et al.*, 1996; Zar *et al.*, 2007). Given the higher cost of oral vancomycin therapy and concern about selection for

vancomycin-resistant enterococci, metronidazole is preferred as the initial agent of choice (Surowiec *et al.*, 2006; Durai, 2007; Owens, 2007). However, reports of metronidazole inferiority in treating severe disease have recently emerged (Musher *et al.*, 2005; Zar *et al.*, 2007; Al-Nassir *et al.*, 2008). Adjunctive and alternative therapeutic approaches are being investigated. Antimicrobial agents, e.g. Ramoplanin and Rifaximin, human monoclonal antibodies as toxin neutralizing agent and vaccines against *C. difficile* are being evaluated (Aslam *et al.*, 2005; Hedge *et al.*, 2008). Furthermore, use of intravenous gamma globulin administration (Leung *et al.*, 1991; Salcedo *et al.*, 1997) and probiotics (McFarland, 2006) can be considered.

C. difficile infection is acquired fecal-orally through endospores resistant towards heat (< 120°C), alcohol based disinfectants and broad spectrum antibiotics. It is considered as main anaerobic pathogen causative for nosocomial infections, however, incidence of community-acquired *C. difficile* infections has increased within the last years.

The risk of enhanced *C. difficile* colonization correlates with advanced age, severe underlying disease of the host and a compromised immune system (Frost *et al.*, 1998).

1.2 *Clostridium difficile* strains and toxinotypes

Several typing methods are developed to differentiate *Clostridium difficile* strains. Initial molecular methods involved plasmid analysis and whole-genome restriction enzyme analysis (REA). REA typing is based on Hind III restriction of genomic DNA leading to a strain specific fragment pattern. However, since this process is very time-consuming and the REA pattern difficult to interpret, it is not routinely used (Rafferty *et al.*, 1998). Rather, PCR ribotyping is used to detect specific sequence polymorphisms enabling the differentiation of strains of the same species. This method relies on amplification of the 16S-23S rRNA intergenic spacer region resulting in different PCR ribotype patterns reflecting strain-dependent variations in the possession of different rRNA alleles (Cartwright *et al.*, 1995).

Clostridium difficile strains are classified into toxinotypes (I-XXIV) which are defined by changes in the pathogenicity locus (Rupnik *et al.*, 1998). Toxinotypes are differentiated by a method, designated Toxinotyping, which is based on RFLP-PCR (**R**estriction **F**ragment **L**ength **P**olymorphism). Therefore, parts of the toxin genes are amplified and the resulting PCR fragments are scanned for length polymorphisms and digested with different restriction enzymes to monitor restriction fragment length polymorphisms (RFLPs). According to the observed patterns a strain is grouped within a given toxinotype (Rupnik *et al.*, 1998; Rupnik *et al.*, 2008). Toxinotype 0 strains contain a pathogenicity locus identical to the reference strain VPI10463 whereas variant *C. difficile* strains are defined by changes in the pathogenicity locus resulting in altered toxin production. Thus, *C. difficile* is a very

heterogeneous species with strains possessing different toxin production types according to the combination of the three toxins: TcdA, TcdB and the binary toxin CDT.

Among the reference strain *C. difficile* VPI10463 the virulent and drug-resistant strain 630 and different variant strains were used in this study (Tab. 1.1). *Clostridium difficile* strain 196 (PCR ribotype 027) has been identified in recent nosocomial outbreaks and infections with increasing incidence and severe disease. It presents higher pathogenicity presumably because of increased toxin production and a characteristic antibiotic resistance profile (Pepin *et al.*, 2004; McDonald *et al.*, 2005; Warny *et al.*, 2005). Its high toxin yield may partially be caused by a frameshift mutation in *tcdC*, encoding a negative regulator of TcdA and TcdB expression (Mani and Dupuy, 2001; Matamouros *et al.*, 2007; Wolff *et al.*, 2009).

C. difficile strain	Toxin producing type	Toxinotype
VPI10463	A+ B+ CDT-	0
630	A+ B+ CDT-*	0
1470**	A- B+ CDT-	VIII
196	A+ B+ CDT+	III

Tab. 1.1: List of *Clostridium difficile* strains and the respective toxin producing- and toxinotypes. The toxin producing type of the *C. difficile* strains expresses exhibition of the toxins A (TcdA), B (TcdB) and CDT (binary toxin). Additional the toxinotype is given which classifies *C. difficile* strains and is defined by changes in the pathogenicity locus. (*The genes encoding CDT are present as pseudogenes exhibiting stop codons and frame-shift mutations; ** Source: Pituch *et al.*, 2007)

1.3 *Clostridium difficile*: Genome and pathogenicity locus

Sequencing of the genome of *C. difficile* strain 630 has recently been completed at the Sanger Institute UK (http://www.sanger.ac.uk/Projects/*C_difficile*/, 10.05.09). It consists of a circular chromosome containing 4,290,252 bp and a plasmid with 7881 bp. Only 15 % of *C. difficile* coding sequences (CDSs) are shared with other sequenced clostridia species (e.g. *C. botulinum*, *C. tetani* and *C. perfringens*) encoding mainly essential functions. Interestingly, 50 % of the CDSs are unique to *C. difficile* basically encoding accessory proteins and mobile elements (Sebaihia *et al.*, 2006). *C. difficile* 630 revealed a large proportion (11%) of mobile genetic elements, mainly in the form of conjugative transposons (Sebaihia *et al.*, 2006). Pathogenic *C. difficile* strains possess a 19.6 kb chromosomal genetic locus, designated as pathogenicity locus (PaLoc).
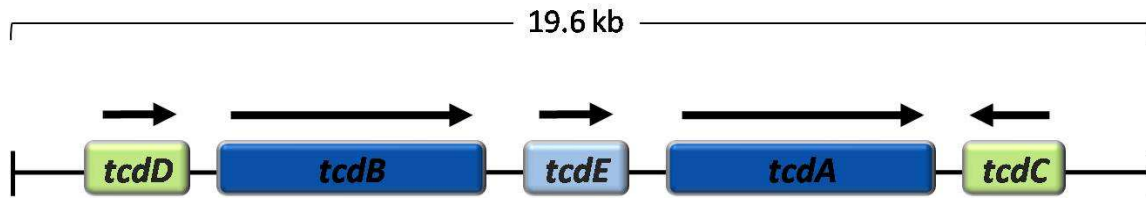
Fig. 1.2: Pathogenicity locus (PaLoc) of *Clostridium difficile*. The genes for the toxins TcdA and TcdB (*tcdA* and *tcdB*) are part of a 19.6 kb genetic locus including additional three open reading frames designated *tcdC*, *tcdD* and *tcdE*. The direction of the arrows reflects orientation of transcription.

The PaLoc harbors the genes encoding the pathogenicity factors TcdA and TcdB and is a prerequisite for virulence. In nontoxigenic strains the pathogenicity locus is replaced by a 115 bp fragment (Hammond and Johnson, 1995; Braun *et al.*, 1996), suggesting that the PaLoc represents a mobile genetic element. However, investigations did not support this hypothesis since tRNA genes are missing which often account for integration sites of genetic elements. In addition, no short *inverted terminal repeats* were identified usually involved in the transposition process (Braun *et al.*, 1996).

Among the genes for the toxins TcdA and TcdB, the pathogenicity locus harbors another three genes of partially unknown function with regard to *C. difficile* virulence. The *tcdD* gene, located upstream of *tcdB*, was demonstrated to promote up-regulation of TcdA- and TcdB synthesis by encoding an alternative sigma factor crucially involved in transcription initiation (Missiakas and Raina, 1998; Mani and Dupuy, 2001; Mani *et al.*, 2002; Karlsson *et al.*, 2003). Conversely, a negative regulatory function has been proposed for *tcdC* which is positioned downstream of *tcdA* and is transcribed in opposite direction (Hundsberger *et al.*, 1997; Hammond *et al.*, 1997). *TcdE* is an open reading frame located between the genes for the toxins TcdA and TcdB and further described in the following section.

A third toxin, not related to TcdA and TcdB, was identified in certain *C. difficile* strains, named binary toxin CDT. CDT is member of the binary toxins produced by *Clostridium perfringens* (type E) and *Clostridium botulinum* (types C and D) (Rupnik *et al.*, 2003b; Rupnik, 2008). Binary toxins are ADP-ribosyltransferases directly modifying actin molecules (Perelle et al., 1997). Its role in pathogenesis is still controversially discussed (Geric *et al.*, 2006).

1.4 *Clostridium difficile* TcdE

The small open reading frame *tcdE* is part of the pathogenicity locus of *Clostridium difficile* and consists of about 500 bp. It is located between the genes encoding the pathogenicity factors TcdA and TcdB, more precisely 122 bp downstream of the *tcdB* stop codon and 727 bp upstream of the *tcdA* start codon (Hammond and Johnson, 1995). *TcdE* encodes the

putative protein TcdE consisting of 166 amino acids with a deduced molecular weight of 19 kDa (Tan *et al.*, 2001). TcdE was predicted to be highly hydrophobic exhibiting three transmembrane domains which are connected via hydrophilic regions. Transmembrane prediction was performed using the Dense Alignment Surface method (Stockholm University, accessible on Expasy Tools) which discriminates between soluble and membrane proteins by searching for α-helical regions within the submitted protein sequence.
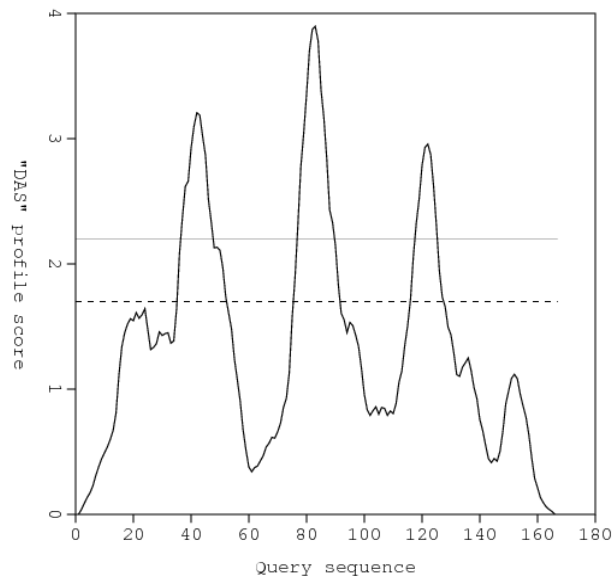
Fig. 1.3: Hydrophobicity plot of *Clostridium difficile* TcdE. Prediction of transmembrane regions in *Clostridium difficile* TcdE using the Dense Alignment Surface method (Stockholm University). TcdE is predicted to exhibit three transmembrane domains connected by hydrophilic stretches. The area above the horizontal lines indicate the hydrophobic regions of the TcdE protein (solid line: strict cut off, dashed line: loose cut off). The x-axis represents the amino acid residues.

Amino acid sequence analysis further revealed a short hydrophilic stretch at the N-terminus and charge-rich residues at the C-terminus of the protein (Tan *et al.*, 2001).

Although TcdE sequence was analyzed in 1990 (Dove *et al.*, 1990) the function of the hydrophobic protein is yet to be defined. Structural similarities to holin proteins and the observation that TcdE expression in *Escherichia coli* resulted in a loss of culture turbidity raised the assumption of a holin-like function of TcdE (Wang *et al.*, 2000; Tan *et al.*, 2001). Transcription analysis revealed a polycistronic transcription of the PaLoc genes *tcdA,B,D,E* in addition to the monocistronic transcription of the genes *tcdA and tcdB* indicating that TcdC-E are involved in *C. difficile* pathogenicity as well. Among transcriptional regulation of TcdE via the *tcdD*- and *tcdB* promoters, *tcdE* was supposed to have an own promoter since promoter elements, like the -35 and -10 boxes match well with those of the deduced *tcdA/B* promoters. Additionally, RT-PCR approaches revealed that mRNAs of *tcdA*, *tcdB* and *tcdE* are produced during the late exponential growth phase of *C. difficile* indicating a simultaneous expression of TcdE and TcdA/B after the stationary phase of growth (Hundsberger *et al.*, 1997).

1.5 Holins

Holins are small bacteriophage-encoded membrane proteins controlling the length of an infection cycle of tailed phages. During phage assembly, holin molecules accumulate in the cytoplasmic membrane without detectable effect on the host (Wang *et al.*, 2000; Gründling *et al.*, 2001; Park *et al.*, 2007). At a precisely scheduled time, which is programmed into their primary structure, holins trigger disruption of the cytoplasmic membrane by oligomerization and forming lethal holes within the membranes. Subsequently, a second class of bacteriophage-encoded proteins, the muralytic endolysins, pass these pores and cleave the peptidoglycan polymer causing cell lysis (Gründling *et al.*, 2001; Park *et al.*, 2006).

The group of holins is extremely diverse but on the basis of primary structure and membrane topology two classes are distinguished. Class I holins, e.g. lambda holin (S^λ), exhibit usually more than 90 amino acid residues and possess two or rather three transmembrane domains (TMD). Analysis of the charge distribution assumed a periplasmic N-terminus and a cytosolic C-terminus. Class II holins, the prototype is the S protein from lambdoid phage 21 (S^{21}), are 75 residues or less in length and exhibit two putative TMDs with both termini located in the cytosol (Bonovich and Young, 1991; Young, 1992; Young and Bläsi, 1995) (Fig. 1.4).
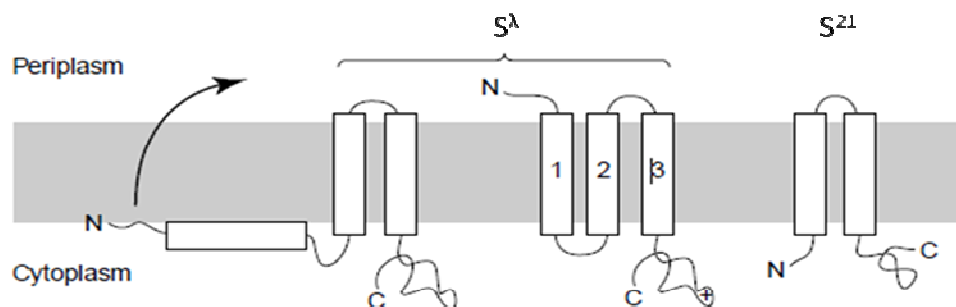
Fig. 1.4: Putative transmembrane topologies of the holins S^λ and S^{21} (Young *et al.*, 2000)**.**

Interestingly, genetic analysis of λ-phage revealed a second start codon (Met) separated from the first by only one lysine residue. Both Met codons are utilized for translation initiation resulting in proteins of different length and function, designated S107 and S105 with respect to their length in amino acid residues (Bläsi *et al.*, 1989; Bläsi *et al.*, 1990; Wang *et al.*, 2000). S105 is the active holin of λ-phage, whereas the two amino acids longer S107 acts as its inhibitor, named the antiholin. The inhibitory function was proposed to be based on the extra positively charged Lys-residue preventing the first transmembrane domain from integrating into the membrane (Graschopf and Bläsi, 1999). The S107 protein exhibits only two TMDs and dimerizes with and thereby inactivates the holin S105. The proteins S105 and S107 are usually expressed at a ratio of 2:1 (Chang *et al.*, 1995; Bläsi *et al.*, 1996) regulated by an RNA-stem-loop structure, called *sdi* (structure-directed initiation), that determines lysis timing.

Furthermore, previous studies indicated that the lysis causing pore formation assumes oligomerization of S105 to two-dimensional protein aggregates, designated as 'death rafts' (Gründling *et al.*, 2000a; Wang *et al.*, 2003). Fig.1.5 illustrates the proposed process of pore formation. S105 molecules (each circle) accumulate and oligomerize within the cytoplasmic membrane (1. and 2.) developing the 'death raft' (3.). Interaction of the molecules derives via their transmembrane domains. Following opening of an aqueous channel (4.) local depolarization of the cytoplasmic membrane occurs, which triggers conformational changes in the holins and further expansion of the lesion.
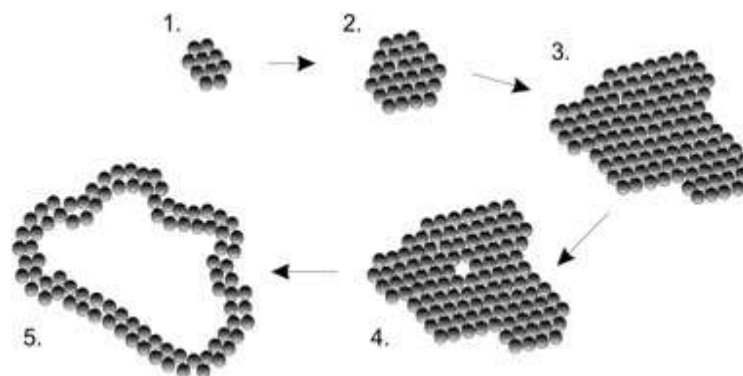
Fig. 1.5: The 'death raft' model for holin lesion formation. Following accumulation and oligomerization of the S105 molecules (1+2, each circle represents a single molecule) formation of the 'death raft' occurs (3). Opening of an aqueous channel (4) triggers conformational changes in the holins resulting in subsequent dispersion of the lesion within the cytoplasmic membrane (Krupovic *et al.,* 2008).

Further investigations revealed that detergent-solubilized λ-holin formed large ring-shaped structures which stacked onto each other to establish larger tubular assemblies. Examinations of the S105 assemblies by means of cryo-Electron microscopy exposed a three-dimensional structure of a λ-holin ring-dimer (Fig. 1.6, upper panel) with an outer diameter of 23 nm and an inner diameter of 9 nm. The height of each ring monomer (4 nm) closely matched the thickness of a lipid bilayer (Fig. 1.6, lower panel) supporting the 'death raft' model (Savva *et al.*, 2008).
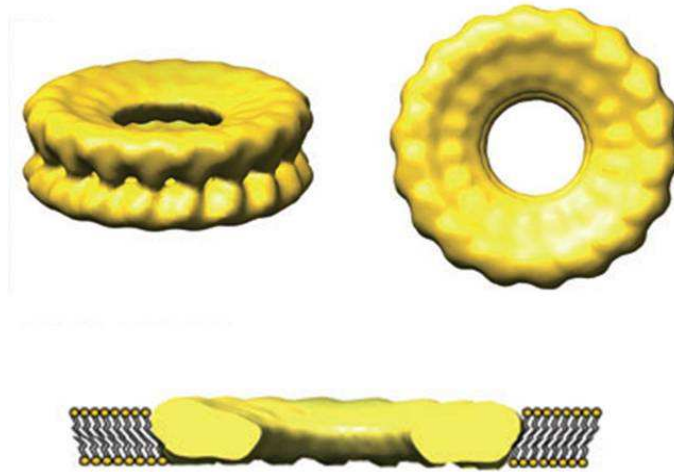
Fig. 1.6: Three-dimensional reconstruction of a λ-holin ring-dimer on the basis of Electron microscopy. Detergent-solubilized λ-holin formed large, well-dispersed ring-shape structures stacking onto each other to form larger tubular assemblies (upper panel). Since the height of each ring monomer closely matched the thickness of a lipid bilayer (4 nm), a model for integration of a single-ring within the lipid bilayer was proposed (lower panel) (Savva *et al.*, 2008).

1.6 Homologies between *Clostridium difficile* TcdE and holins

Clostridium difficile TcdE is a highly hydrophobic 19 kDa protein of unknown function. Interestingly, amino acid sequence analysis revealed more than 20 % identity and 50 % similarity of TcdE and holins from different bacteriophage species (e.g. 23 % identity and 54 % similarity to holin 87 of *Streptococcus thermophilus* bacteriophage Sfi19 and 25 % identity and 52 % similarity to *Bacillus subtilis* bacteriophage B103 holin). The highest homology between TcdE and holins was detected within the C-terminus of TcdE flanked by amino acids 121 and 166 (Tan *et al.*, 2001).

Among sequence homologies, *Clostridium difficile* TcdE and bacteriophage-encoded holins share structural similarities based on resemblance in the distribution of hydrophilic and hydrophobic amino acids. Holins are small membrane-spanning proteins possessing a hydrophilic N-terminus and a highly charged C-terminus (Young and Bläsi, 1995). Consistent with this, on the basis of hydrophobicity analysis TcdE was predicted to exhibit three transmembrane domains. Furthermore, amino acid sequence analysis of TcdE also revealed a hydrophilic stretch at the N-terminus and a charge-rich C-terminus (Tan *et al.*, 2001).

Interestingly, additional to striking resemblance in sequence and structure, TcdE was shown to exhibit holin-like functional properties since TcdE expression in *Escherichia coli* resulted in a sudden halt of bacterial growth and gradual loss of culture turbidity (Tan *et al.*, 2001).

An important characteristic of holins is the dual start motif resulting in proteins of different length and function, a holin and its inhibitor. Analysis of TcdE nucleic acid sequence exposed

two additional ATG start codons contributing to amino acids 25 and 27. Furthermore, an alternative ribosome binding site was found upstream of both the first (GGTGG) and third (GGAGG) start codons of *tcdE* (Dove *et al.*, 1990) indicating an existence of a dual start motif in *tcdE* mRNA as well. The deduced molecular weights of the putative proteins initiating from the first and third start codons are 19 kDa and 16 kDa, respectively.

Since *tcdE* was shown to be transcribed polycistronically with the *tcdA* and *tcdB* genes, the putative TcdE protein was attributed to play a crucial role in the pathogenicity of *C. difficile* (Von Eichel-Streiber *et al.*, 1987; Hundsberger *et al.*, 1997). On the one hand, TcdE was postulated to have regulatory function with respect to the toxin genes *tcdA* and *tcdB* (Dove *et al.*, 1990). Otherwise, Von Eichel-Streiber and Sauerborn hypothesized that TcdE facilitates the release of the pathogenic toxins, due to its holin-like feature in *E. coli* and a lack of signal peptide for extracellular secretion regarding TcdA and TcdB (Von Eichel-Streiber and Sauerborn, 1990).

The question, however, cannot appropriately be addressed without a specific functional genetic knockout, a technique that was not established at that time for Gram positive bacteria.

2. Aim of the thesis

The small open reading frame *tcdE* within the pathogenicity locus of *Clostridium difficile* is located between the genes for the pathogenic toxins TcdA and TcdB. Function and mode of action of the putative hydrophobic protein TcdE are unknown so far. Since no export mechanism for TcdA and TcdB is known and sequence homologies between TcdE and bacteriophage encoded holins were identified TcdE is supposed to facilitate release of the toxins from *C. difficile* into the extracellular environment. Alternatively, TcdE is hypothesized to be involved in colonization of *C. difficile* by affecting intestinal commensals or to act as an additional pathogenicity factor. The question of TcdE function cannot appropriately be addressed without a functional specific genetic knockout, a technique which was established no more than a few years ago.

The aim of this study was to identify a regulatory or pathogenic impact of TcdE and to evaluate its role in *C. difficile* virulence. Therefore, the following aspects were investigated:

Structure-function relationship of TcdE. TcdE deletion mutants have to be generated. The functional outcome of expression in *E. coli* has to be analyzed to identify functional domains of the protein. Furthermore, the putative holin-like dual start motif has to be mutated to examine its role in TcdE specific mode of action.

Investigation of a potential pathogenic impact. To evaluate the role of TcdE in *C. difficile* pathogenicity, the influence of TcdE on isolated epithelial mitochondria and on the intact cell system have to be analyzed.

Consequences of TcdE knockout in C. difficile. Insertional inactivation of *tcdE* has to be performed to analyze alterations in *C. difficile* specific characteristics with respect to bacterial growth, sporogenesis and toxin release. The specific TcdE knockout reveals unambiguous information about involvement of TcdE in virulence.

3. Materials and methods

3.1 Materials

T7 Express *lysY/I^q* Competent *Escherichia coli* (New England Biolabs); pQE30 vector (Qiagen, Germany); pcDNA3.1 vector (Invitrogen); pMTL007C-E2 (kindly provided by N. Minton, University of Nottingham); Oligonucleotides were synthesized by Operon, Germany; QuickChange XL site-directed mutagenesis kit (Stratagene, Germany); Restriction endonucleases, T4 DNA ligase and alkaline phosphatase were purchased from New England Biolabs; Pwo-Polymerase from Peqlab Biotechnologie GmbH (Germany); Fugene HD transfection reagent was from Roche (Germany); cell culture supernatant of α-myc secreting hybridoma cells was kindly provided by B. Sodeik (Institute of Virology, Hannover Medical School); Alexa Fluor 568 conjugated phalloidin was purchased from Molecular Probes (OR, USA); peroxidase-conjugated goat anti-rabbit IgG (Rockland, PA, USA);

antigen	host	monoclonal	company/ source
TcdA	rabbit	no	Institute of Toxicology, MHH
TcdB	rabbit	no	Institute of Toxicology, MHH
TcdE (aa 134-166)	rabbit	no	this study
cytochrome *c*	mouse	yes	BD Biosciences Pharmingen, NJ, USA
cleaved caspase-3	rabbit	yes	Cell Signalling, MA, USA
myc	mouse	yes	kindly provided by B. Sodeik (Institute of Virology, Hannover Medical School)

Tab. 3.1. Primary antibodies

host	animal	conjugated	company
goat	rabbit	peroxidase	Rockland, PA, USA
goat	mouse	peroxidase	Rockland, PA, USA
goat	rabbit	Alexa Fluor 555	Molecular Probes, OR, USA
goat	mouse	Alexa Fluor 488	Molecular Probes, OR, USA

Tab. 3.2. Secondary antibodies

3.2 Methods

3.2.1 Microbiological methods

3.2.1.1 Bacterial strains and culture

Clostridium difficile strains VPI10463 (Accession-No. X92982), 1470, 630 (Acc.-No. AM180355), 630Δ*tcdE*-234a (this study) and the hypervirulent strain 196 (Acc.-No. L76081) were grown in Brain Heart Infusion (BHI) broth at 37°C in an anaerobic gas jar.

T7 Express *lysY/I^q* Competent *Escherichia coli* serving as cloning and expression hosts, respectively, were grown in Luria-Bertani (LB) medium supplemented with ampicillin (100 mg/L).

3.2.1.2 Generation of bacteria growth profiles

Transformed *E. coli* or different *C. difficile* strains were grown in their respective media. At indicated time points 750 µl of liquid culture were taken and subjected to photometry to determine the optical density at 600 nm (OD_{600}). The photometer was calibrated to $OD_{600} = 1$ corresponding to 5×10^8 cells per ml.

3.2.1.3 *C. difficile* cultivation and toxin expression

(A) 10 ml scale

Overnight cultures of *C. difficile* were pelleted and resuspended in fresh BHI broth to exclude distortion by toxins and spores at the initial values. The main culture was then inoculated with bacteria suspension with a volume calibrated to the respective optical density. The different *C. difficile* strains were cultivated for 0, 8, 24, 48 and 72 h and 10 ml of bacteria culture were pelleted at the respective time point by centrifugation for 10 min at 4,000 g. The supernatants were collected and chloroform methanol precipitation of 800 µl was performed according to Wessel and Flugge *et al.* (1984). Finally, the entire protein pellet harbouring the toxins A and B were solubilised in 50 µl PBS, sonicated (1 x 5 s, Cycle 50 %, Power 10 %) and laced with 5 x Lämmli. Protein solution was bisected and subjected to SDS-PAGE and Western blot analysis to detect the TcdA and TcdB contents. The bacteria pellet containing TcdE was solubilised in 150 µl PBS supplemented with 5 mg/ml lysozyme and 1 mM AEBSF and sonicated (1 x 1 min, Cycle 90 %, Power 40 %) after incubation for 1 h at 37°C. Finally, the lysate was subjected to SDS-PAGE after calibration to the respective optical densities at time point of harvest. Western blot analysis with α-TcdE enabled the detection

of TcdE levels in a time dependent manner. Kodak software was used for densitometric analysis.

(B) 500 ml scale

500 ml BHI was inoculated either with *C. difficile* strain 630Δ*erm* or with the TcdE-knockout strain cdi630Δ*tcdE* and cultivated for 24 h. Bacteria were harvested by centrifugation at 7,000 g for 20 min and lysed in 10 ml 50 mM Tris-HCl (pH 8.0), 2 mM MgCl$_2$, 10 % glycerol, 2 mM dithiotreitol (DTT) and 1 mM AEBSF using French Press. Following centrifugation at 15,000 g for 20 min pelleted cell debris was resuspended in 2 ml lysis buffer mentioned above, supplemented with 2 % Triton X-100 and incubated for 30 min at 4°C to solubilise TcdE. 5 x Lämmli was added to 10 µl of suspension and SDS-PAGE and Western blot analysis with α-TcdE were performed.

3.2.1.4 Gram staining of *C. difficile*

The different strains of *C. difficile* were cultivated for 0, 8, 24, 48 and 72 hours. 500 µl of the cells were pelleted by centrifugation at 10,000 g for 2 min. After discarding the supernatants the pellets were solubilised in 20 µl BHI broth and streaked on glass slides. Afterwards, Gram staining was performed according to Lillie (1977) and the sections were subjected to light microscopy.

3.2.1.5 Generation of a TcdE deficient *C. difficile* mutant

The *tcdE* gene in *C. difficile* strain 630Δ*erm* (Hussain *et al*., 2005) was disrupted by directed insertional inactivation using a bacterial group II intron according to Heap *et al*. (2007). In brief, one-tube SOE PCR (Splicing by Overlap Extension PCR) was performed to amplify a 353 bp product containing the modified IBS, EBS1d and EBS2 sequences which are specific for the taget gene *tcdE* and responsible for intron targeting. The target sites were identified and specific intron re-targeting primers were designed by means of a computer algorithm (Perutka *et al*., 2004) which is part of the Targetron Gene Knockout system kit (http://www.sigmaaldrich.com). The following primers were used: IBS: AAAAAAGCTTAT AATTATCCTTAAATATCCATGCTGTGCGCCCAGATAGGGTG; EBS1d: CAGATTGTACAA ATGTGGTGATAACAGATAAGTCCATGCTATTAACTTACCTTTCTTTGT; EBS2: TGAACGC AAGTTTCTAATTTCGATTATATTTCGATAGAGGAAAGTGTCT. The amplified targeting region was ligated via HindIII and BsrGI restriction sites into the plasmid pMTL007C-E2 and transformed in *E. coli* donor CA434. Plasmid pMTL007C-E2 exhibits a Retrotransposition-activated selectable marker (RAM) coding for an erythromycin resistance which is activated after successful integration of the modified intron into the right target site. The retargeted

intron, named pMTL007C-E2:cdi-*tcdE*-234a according to the existing convention (Karberg *et al*., 2001), was then transferred in *C. difficile* 630Δ*erm* via conjugation. Classification "234a" indicates insertion of the modified intron at position 234 of the *tcdE* gene in antisense direction. Finally, the transconjugants were re-streaked on BHI plates supplemented with 2.5 µg/ml erythromycin to select for integrants and 250 µg/ml cycloserine and 8 µg/ml cefoxitin to select against the *E. coli* donor.

3.2.2 Molecular biological methods

3.2.2.1 Generation of TcdE constructs

The *tcdE* gene was amplified from *C. difficile* (VPI 10463, Accession No. X92982) genomic DNA using the primers listed in Tab. 3.3 and Tab. 3.4. PCR was performed in 50 µl with 200 ng DNA, 300 nM of each primer, 250 µM dNTPs, 1x complete reaction buffer for Pwo polymerase and 2.5 U Pwo DNA Polymerase. The PCR conditions were the following: one initial cycle for denaturation at 95°C for 1 min, 28 cycles of denaturation at 95°C for 15 s, annealing at 55°C for 30 s and extension at 70°C for 1 min followed by a final extension phase at 70°C for 10 min. The PCR products were digested by BamHI and HindIII (pQE30) respectively XhoI and BamHI (pcDNA3.1) and then inserted into the corresponding plasmid vectors. Transformation and protein expression occurred in T7 Express *lysY/I*^{q} competent *E. coli*. A fusion construct of N- and C-terminus (TcdE NC) was generated on the basis of commercial oligonucleotides which were ligated successively in pQE30 connected by a glycine linker.

Primer	bp	Sequence
TcdE wt (s)	1-501	5' AGTCACTCGAGCGATGCACAGTAGTTCACCTTTTTATATTTC
TcdE wt (a)		5' AGTCGGATCCCTTTTCACCCTTAGCATTCATTTCATC

Tab.3.3: Primers used for cloning into pcDNA3.1 vector

Primer	bp	Sequence
TcdE wt (s) TcdE wt (a)	1-501	5′AGTCGGATCCATGCACAGTAGTTCACCTTTTTATATTTC 5′AGTCAAGCTTCTTTTCACCCTTAGCATTCATTTCATC
TcdEΔN (s) TcdEΔN (a)	79-501	5′AGTCGGATCCATGACAATATCTTTTTTTATCAG 5′AGTCAAGCTTCTTTTCACCCTTAGCATTCATTTCATC
TcdEΔC (s) TcdEΔC (a)	1-397	5′AGTCGGATCCATGCACAGTAGTTCACCTTTTTATATTTC 5′AGTCAAGCTTCTACATATTTTTTTAATATACTTACACTTTCATA
TcdEΔNΔC (s) TcdEΔNΔC (a)	79-397	5′AGTCGGATCCATGACAATATCTTTTTTTATCAG 5′AGTCAAGCTTCTACATATTTTTTTAATATACTTACACTTTCATA
TcdE N (s) TcdE N (a)	1-79	5′GATCAATGCACAGTAGTTCACCTTTATATTTTAATGGTAACAAAAT ATTTTTTTATATAAACCTAGGGGGCGTTATGAATATGGGTGGTGGTGG TGGATCCGGTGGTAAGCTTT 5′AGCTAAAGCTTACCACCGGATCCACCACCACCACCCATATTCATAA CGCCCCCTAGGTTTATATAAAAAAATATTTTGTTACCATTAAAATATA AAGGTGAACTACTGTGCATT
TcdE C (s) TcdE C (a)	397-501	5′GATCTAATATGTGCTTATGTGGATTACCAGTACCTAAGAGATTAAA GGAAAAAATAGTAGTTTTACTAGATGCAATGACAGATGAAATGAATGC TAAGGGTGAAAAGGGATCCGGTGGTAAGCTTT 5′AGCTAAAGCTTACCACCGGATCCCTTTTCACCCTTAGCATTCATTT CATCTGTCATTGCATCTAGTAAAACTACTATTTTTTCCTTTAATCTCT TAGGTACTGGTAATCCACATAAGCACATATA

Tab. 3.4: Primers used for cloning into pQE30 vector

3.2.2.2 Generation of an N-terminal deletion mutant pcDNA3.1-TcdEΔN in a single cloning step

The generation of the N-terminal deletion mutant pcDNA3.1-TcdEΔN was performed in a single cloning step according to Makarova *et al.* (2000). The PCR was accomplished in 50 μl with 100 ng pcDNA3.1-TcdE as DNA template, 200 nM of each primer (Tab. 3.5.), 200 μM dNTPs, 1x buffer for Pfu Polymerase and 2.5 U Pfu DNA Polymerase. The following PCR conditions were used: one initial cycle for denaturation at 95°C for 3 min, 18 cycles of denaturation at 95°C for 15 s, annealing at 65°C for 1 min and extension phase at 68°C for 12 min followed by a final extension at 68°C for 15 min. Finally, digestion of methylated parental DNA with 1 μl Dpn I (10 U/μl) for 1 h at 37°C occurred followed by transformation in T7 Express *lysY/I^q* competent *E. coli*.

Primer	bp	Sequence
TcdEΔN (s) TcdEΔN (a)	79-501	5'CGGGCCCTCTAGACTCGAGCGATGACAATATCTTTTTTATCAGAGCATA 5'TATGCTCTGATAAAAAGATATTGTCATCGCTCGAGTCTAGAGGGCCCG

Tab. 3.5: Primers used for generation of pcDNA3.1-TcdEΔN in a single cloning step

3.2.2.3 Site-directed mutagenesis

Site-directed mutagenesis within the Shine-Dalgarno sequence or start codons of TcdE was performed to investigate a putative dual start motif. Mutagenesis was carried out as described by the manufacturer's instructions. The applied primers are listed in Tab. 3.6. Wildtype TcdE in pQE30 was used as template for PCR.

Primer	Short name	Sequence
TcdE G22L (s) TcdE G22L (a)	SD I	5'ATATAAACCTATTAGGCGTTATGAATATGACAATATC 5'GATATTGTCATATTCATAACGCCTAATAGGTTTATAT
TcdE G22L G23V (s) TcdE G22L G23V (a)	SD II	5'ATATAAACCTATTAGTCGTTATGAATATGACAATATC 5'GATATTGTCATATTCATAACGACTAATAGGTTTATAT
TcdE M25A M27C (s) TcdE M25A M27C (a)	Met	5'CCTAGGAGGCGTTGCGAATTGCACAATATCTTTTTTATC 5'GATAAAAAGATATTGTGCAATTCGCAACGCCTCCTAGG

Tab. 3.6: Primers used for site-directed mutagenesis

3.2.3 Biochemical methods

3.2.3.1 Expression of recombinant protein

(A) 50 ml scale

50 ml *E. coli* cultures carrying the indicated plasmids were grown at 37°C with shaking at 175 rpm until the OD_{600} was 0.5. Protein expression was induced by the addition of 1 mM isopropyl-β-D-thiogalactoside (IPTG). Growth profiles were monitored for up to 6 h respectively 24 h by measuring the OD_{600}. For time-course analysis of protein expression 1.5 ml samples were harvested at different time points and pelleted by centrifugation at 10,000 g for 2 minutes. The supernatant was discarded and the pellet was resuspended in 100 µl of 1 x Lämmli supplemented with 1 mM 4-(2- Aminoethyl)-benzensulfonylfluorid (AEBSF).

(B) 1l scale

T7 Express *lysY/I^q* competent *E. coli* harbouring the vector plasmid or its derivatives pQE30-TcdE and pQE30-TcdEΔN were cultivated in 1 l scale and induced as described above. After 1 h expression bacteria were pelleted at 7,000 g for 20 min and lysed in 50 mM Tris-HCl (pH 8.0), 2 mM MgCl₂, 10 % glycerol, 2 mM dithiotreitol (DTT) and 1 mM AEBSF using French Press. The bacterial lysate was centrifuged at 15,000 g for 30 min to pellet the cell debris. The supernatant containing the soluble fraction of TcdE was sterile filtered (0.22 µm) and directly used for cytochrome *c* release assay.

3.2.3.2 Generation of specific antibody

The TcdE C-terminus DNA (397-498 bp) was cloned in pQE30 3-fold in succession linked by glycine residues and expressed in T7 Express *lysY/I^q* competent *E. coli*. Immunization of a female newzeeland rabbit was performed after standard protocol using affinity purified immunogen (amino acid sequence: MCLCGLPVPKRLKEKIVVLLDAMTDEMNAKGEKGGG MCLCGLPVPKRLKEKIVVLLDAMTDEMNAKGEKGGGMCLCGLPVPKRLKEKIVVLLDTDE MNAKGEK) in Freud's adjuvant. First immunisation was performed with 100 µg of protein followed by a single boost after four weeks. Blood was collected three weeks after boost immunisation. Specificity of anti-serum was checked by Western blot using the antigen as control (Permission No. 33-42502-03A351).

3.2.3.3 Isolation of mitochondria and cytochrome *c* release- assay

Mitochondria of Hep2 cells were isolated by differential centrifugation as described by (Perfettini *et al.*, 2002). Hep2 cells were harvested in sucrose buffer (210 mM mannitol, 70 mM sucrose, 1 mM EDTA, 10 mM Hepes (pH 7.5), 100 µM AEBSF, 10 µg/ml leupeptin, 2 µg/ml aprotinin) transferred into a reaction tube and solubilized on ice by repeated suction through a syringe (0.8 x 44 mm). The homogenate was centrifuged at 500 g for 5 min at 4°C to separate mitochondria and larger cell components. The supernatant was used for preparation of the mitochondria enriched fraction by centrifugation at 10,000 g for 30 min at 4°C. The pellet containing the mitochondria was resuspended in 150 µl sucrose buffer to perform cytochrome *c* release-assay. Therefore, mitochondria suspension was incubated with an equal volume of the soluble fraction of TcdE, TcdEΔN and of vector transformed cells, respectively. Following incubation for 2 h at 30°C mitochondria were pelleted at 16,000 g for 15 min. Supernatant and resuspended mitochondria were subjected to SDS-PAGE and Western blot analysis with cytochrome *c*-antibody to detect the ratio of cytochrome *c* in mitochondria and supernatant.

3.2.3.4 ATP determination assay

The ATP determination kit (A22066) by Molecular Probes™ was used to detect ATP released from *E. coli* as a result of bacteriolysis. The bioluminescence assay is based on the reaction of ATP with recombinant firefly luciferase and its substrate luciferin.

The assay was performed according to the manufactor's instructions. In brief, in a 3- fold approach 90 µl of a standard reaction solution containing 25 mM Tricine buffer (pH 7.8), 5 mM $MgSO_4$, 100 µM EDTA, 100 µM sodium azide, 500 µM D-luciferin, 1 µM dithiothreitol (DTT) and 1.25 µg/ml firefly luciferase were combined in a 96-well with 10 µl supernatant of *E. coli* expressing either TcdE or the TcdE mutant Met, respectively. The supernatants were collected 3 h after induction with 1 mM IPTG by spinning 200 µl bacteria culture at 16,000 g for 5 min. Luminescence was monitored after 15 min incubation at 28°C using a Biotek Synergy luminometer.

3.2.3.5 Cytotoxicity assay

Hep2 cells were grown on 24 well chambers for 24 h and exposed to supernatants of the *C. difficile* strains cdi630Δ*erm* and the TcdE-knockout strain cdi630Δ*tcdE* cultivated for 48 h containing the native toxins A and B. Immediately after toxin treatment (0h) and after incubation for 2 h at 37°C cells were subjected to light microscopy and cytopathic effect was quantified as rounded cells per total cells in %. Each result is based on ten independent samples. Values are given as means ± standard deviations.

3.2.4 Immunological methods

3.2.4.1 SDS-PAGE and Western blotting

Protein samples were separated by SDS-PAGE and transferred onto a nitrocellulose membrane using "semi-dry" techniques (17 V, 72 min). After blocking of unspecific binding with 3 % (w/v) bovine serum albumine and 2 % (w/v) nonfat dry milk in TBST (50 mM Tris HCl, 150 mM NaCl, 0.05% (v/v) Tween 20, pH 7.2) the membrane was incubated overnight with the respective primary antibody (Tab. 3.1) in blocking solution at 4°C. After washing thoroughly with TBST, horseradish peroxidase conjugated secondary antibody (Tab. 3.2) was applied for 45 min at RT. Detection was performed by chemiluminescence (Super Signal West Femto, Pierce). KODAK 1D software was used for densitometric analysis.

3.2.4.2 Transfection and immunofluorescence

Hep2 cells were grown on coverslips and plasmid vector pcDNA3.1 or its derivatives pcDNA3.1-TcdE or pcDNA3.1-TcdEΔN were transfected with Fugene HD according to the manufactor's instructions. Twenty-four hours post-transfection, cells were washed with PBS, fixed with 4 % paraformaldehyde/sucrose solution and permeabilized for 5 min with 0.2 % Triton X-100 in PBS. After washing with PBS the coverslips were blocked for 1 h with 10 % BSA in PBS and stained with cleaved caspase-3 antibody (1 : 400 in 1 % BSA in PBS) for 1 h followed by staining with Alexa Fluor 555 conjugated goat anti-rabbit secondary antibody (1 : 200 in 1 % BSA in PBS) for 45 min. After washing with 1 % BSA in PBS second immunofluorescence staining was performed. Therefore cells were incubated with cell culture supernatant of α-myc secreting hybridoma cells for 1 hour at room temperature followed by staining with oregon green conjugated goat anti-mouse secondary antibody (1:2000 in 1 % BSA in PBS) for 45 min. Simultaneously, nuclei were counterstained with DAPI. Filamentous actin was labelled with Alexa Fluor 568 conjugated phalloidin for 45 min (500 nM). Finally, the coverslips were mounted onto glass slides and subjected to confocal laser scanning microscopy (Leica Inverted DM IRE 2). Additionally, control cells were treated 15 h with 1 µm of the protein kinase inhibitor staurosporin which induces apoptosis by activating caspase-3.

3.2.5 Cell biological methods

3.2.5.1 Cell culture

The human epithelial larynx carcinoma cell line (Hep2) was cultivated under standard conditions in Minimal Essential Medium (MEM) with Earle's Salts and L-Glutamine supplemented with 10 % foetal bovine serum (FBS), 100 µM penicillin and 100 µg/ml streptomycin. The cell line was subcultured twice a week. Therefore they were washed once in PBS and incubated in Trypsin-EDTA solution for 5-10 min at 37°C to release the cells. Subsequent to resuspension in their culture medium cells were seeded in flasks or, for transfection experiments, on coverslips in 24 well chambers, respectively.

4. Results

4.1 Influence of *Clostridium difficile* TcdE on bacteria

4.1.1 TcdE induces lysis of *E. coli*

Function and mode of action of *Clostridium difficile* TcdE are unknown. TcdE shows sequence homologies and structural similarities to bacteriophage encoded holins which oligomerize within the host cell membrane forming lethal holes causing cell death of bacteria. Growth profiles of *E. coli* expressing wildtype TcdE were monitored to study TcdE- induced effects on bacteria. TcdE expression in *E. coli* resulted in a sudden loss of culture turbidity subsequently after induction indicating at least a growth inhibiting capacity of TcdE on bacteria. This phenomenon was not observed in *E. coli* transformed with the control vector (Fig. 3.1 [A]). Western blot analysis with specific anti-TcdE serum confirmed the expression of 19 kDa TcdE in induced *E. coli*. Interestingly, an additional 16 kDa protein was detected with a 10-fold higher expression level than the full length protein (Fig. 3.1 [B]).
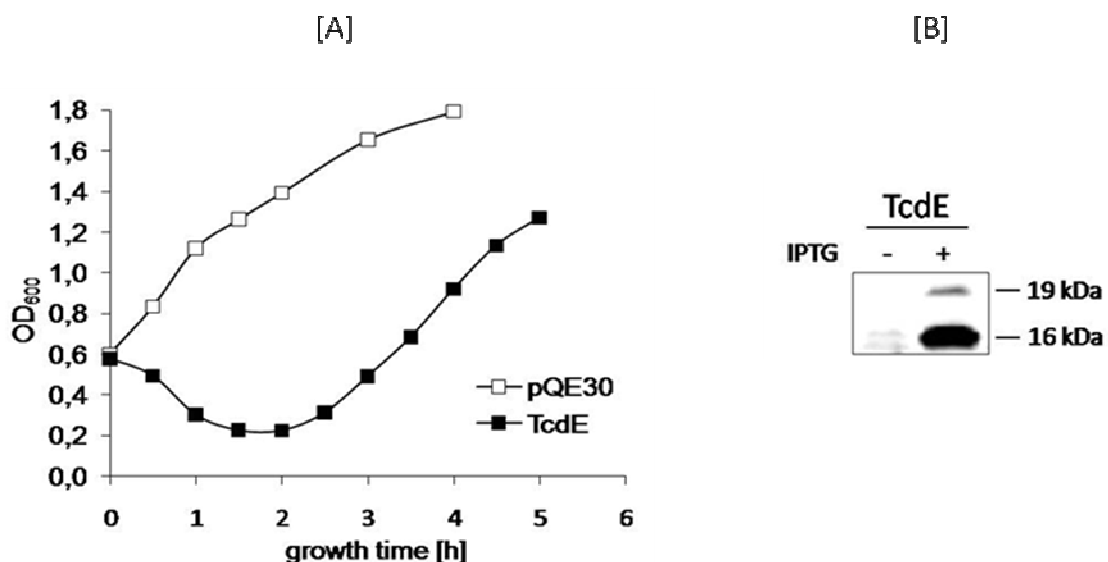
Fig. 4.1: TcdE expression inhibits bacterial growth. [A] The expression of TcdE in *Escherichia coli* resulted in a sudden halt of bacterial growth. Gradual loss of culture turbidity was observed which was not observed in *E. coli* transformed with empty vector. [B] Western blot analysis with α-TcdE confirmed the expression of full length TcdE (19 kDa) in induced *E. coli* after 1 h. Additional a 16 kDa protein was detected with a 10-fold excess.

 As sequence analysis showed, *tcdE* mRNA exhibits two additional AUG start codons contributing to amino acids 25 and 27. The deduced molecular weights of the putative proteins initiating from the first and third start codons are 19 kDa and 16 kDa, respectively. Since holins utilize a dual start motif to produce proteins of different length and function, the expression pattern of TcdE might indicate a similar mechanism. To investigate this hypothesis mutational analysis was performed (Section 4.1.3).

The strong decrease of the optical density to almost 30 % of the initial value implicated bacterial cell lysis. A sensitive method to determine disruption of bacteria is the detection of released ATP in terms of luminescence. Supernatants of *E. coli* expressing either the empty vector or wildtype TcdE for 3 hours were applied to the ATP determination assay. TcdE induced a 10- fold higher ATP release compared to the empty vector which reflected bacteriolysis in consequence of TcdE expression.

Thus, this result confirms a TcdE mediated bacteriolysis.
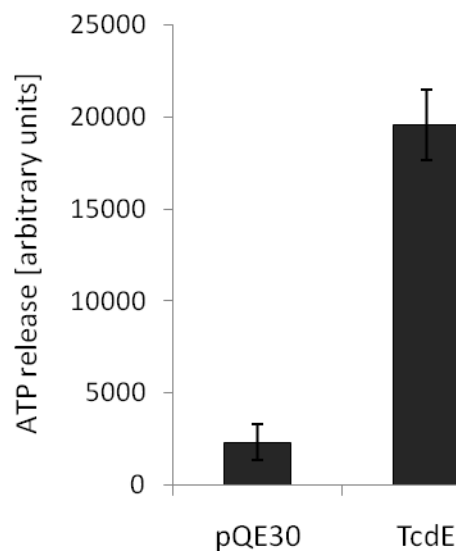
Fig. 4.2: TcdE expression induces bacteriolysis. ATP release from *E. coli* expressing wildtype TcdE was used for detection of bacteriolysis. Supernatants were collected three hours post induction and subjected to ATP determination assay. Luminometry was performed to monitor released ATP. The data verified a TcdE- induced lysis of bacteria according to a tenfold higher ATP-release compared to the vector control. The values are expressed as means ± standard deviation (n=3).

4.1.2 The hydrophobic transmembrane domains are essential for TcdE-induced growth inhibition of bacteria

To investigate putative functional domains for the bacteriolytic property deletion mutants of TcdE were generated. The N-terminal deletion mutant TcdEΔN lacks the N-terminus and

TcdEΔNΔC only consists of the three transmembrane domains. TcdENC reflects a fusion protein of the N- and the C-terminal domains (Fig. 4.3).

Fig. 4.3: Scheme of TcdE deletion mutants. Wildtype TcdE (TcdE wt) exhibits three transmembrane domains, a hydrophilic N-terminus (aa 1-26) and a highly charged C-terminus (aa 133-166). The N-terminal deletion mutant TcdE ΔN lacks the N-terminal region and TcdEΔC accordingly the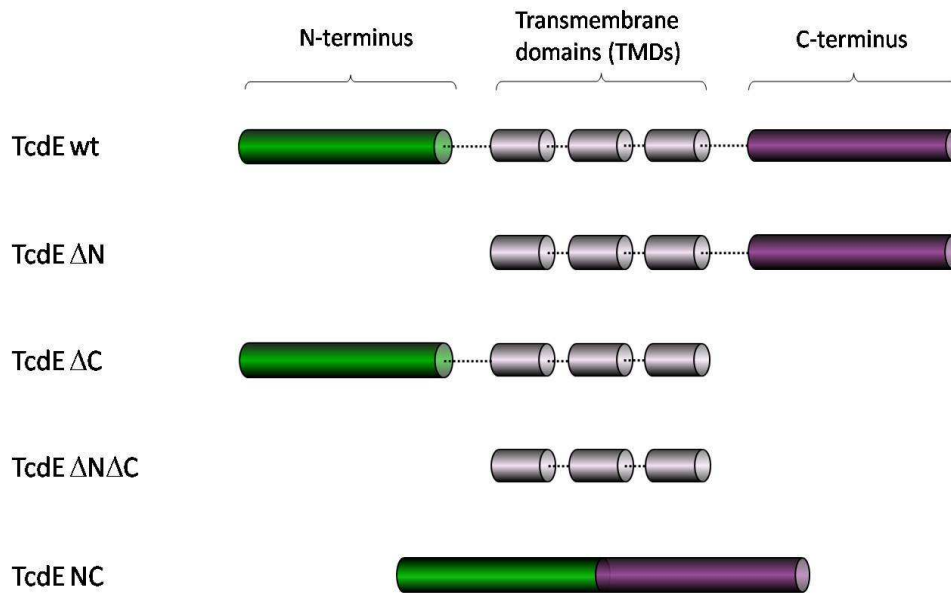 C-terminus. TcdEΔNΔC only consists of the three transmembrane domains and TcdENC reflects a fusion protein of the N- and the C-terminal domains.

Fig. 4.4 shows the growth profiles of *E. coli* expressing wildtype TcdE and the respective mutants. As described above, wildtype TcdE (Fig. 4.4, red squares) induced bacteriolysis monitored by a continuous decrease in optical density following induction. This phenomenon was not observed in *E. coli* transformed with empty vector (Fig. 4.4, black squares). The N-terminal deletion mutant TcdEΔN (Fig. 4.4, blue squares) showed similar effect to that of wildtype TcdE although the OD_{600}-decrease was less pronounced. The fusion protein TcdENC (Fig. 4.4, yellow squares), consisting of the N- and C-terminal regions, did not affect bacterial growth compared to the vector control indicating an essential role for the hydrophobic transmembrane domains of TcdE concerning growth inhibiting. To investigate this hypothesis TcdE mutant ΔNΔC, harbouring only the three transmembrane domains, was expressed. In fact, the expression of TcdEΔNΔC (Fig. 4.4, green squares) resulted in immediate inhibition of bacterial growth. Optical density stagnated at a constant level of $OD_{600} = 0.4$ for at least 5 h following induction revealing the transmembrane domains to be sufficient in inhibition of *E. coli* growth. A C-terminal deletion mutant TcdEΔC was also generated which expression led to an identical growth profile with a congruently developing curve to that of TcdEΔNΔC (not shown). Western blots with α-tcdE antibody confirmed the

expression of wildtype TcdE, TcdEΔN and TcdENC, respectively. Since the TcdE antibody is directed towards the C-terminus of the protein, a method to detect the deletion mutant TcdEΔNΔC was unfortunately missing.
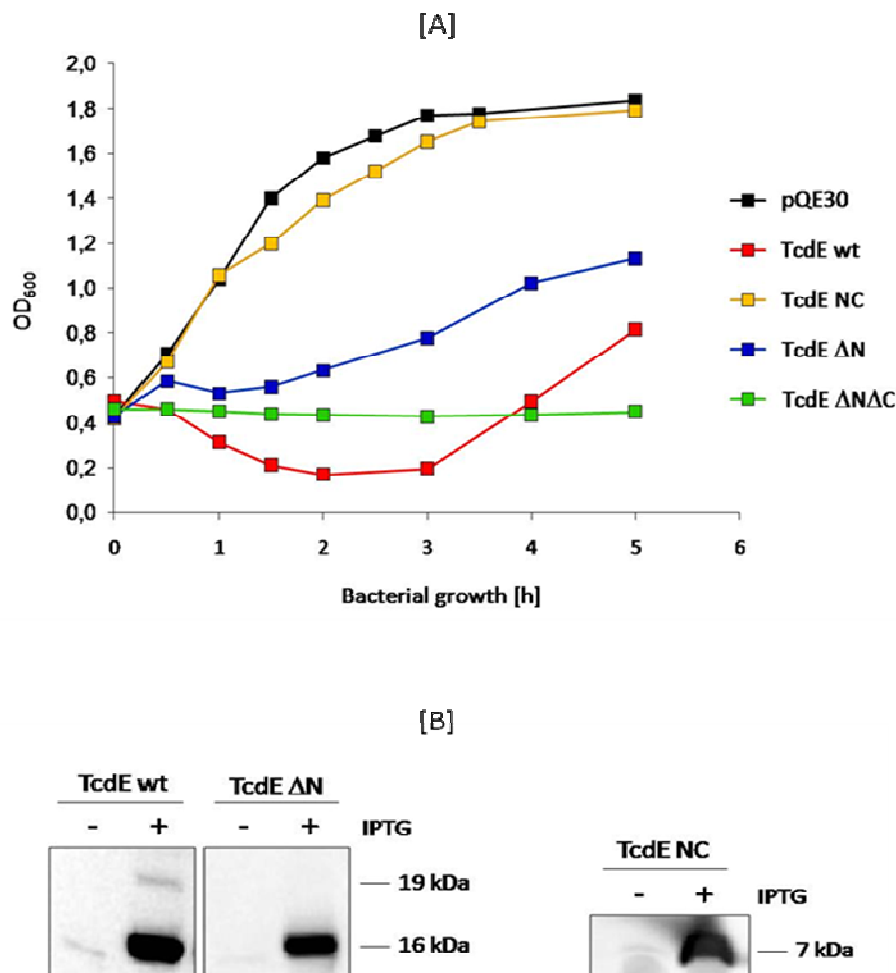

Fig. 4.4: The hydrophobic transmembrane domains are essential for TcdE-induced inhibition of bacterial growth. [A] Growth profiles of *E. coli* expressing wildtype TcdE and TcdE deletion mutants were monitored to further investigate functional domains of the protein. The N-terminal deletion mutant ΔN (blue) lacks the N-terminal region. ΔNΔC only consists of the three transmembrane domains (green) and NC reflects a fusion protein of the N- and the C-terminal domains (yellow). As described, optical density of *E. coli* expressing wildtype TcdE (red) decreased continuously following induction to a value of 0.2. The curve referring to TcdEΔN reflected a similar development, however, only a marginal transient decrease of the optical density was observed. The fusion protein NC did not affect bacterial growth compared to the growth profile of *E. coli* transformed with empty vector (black). Since this observation indicated an essential role for the transmembrane domains concerning inhibitory effects, growth curves of *E. coli* expressing TcdEΔNΔC were monitored. In fact, the hydrophobic transmembrane domains resulted in immediate stagnation of bacterial growth to a constant $OD_{600} = 0.4$ up to 5 h following induction. A C-terminal deletion mutant caused an identical growth profile (not shown). Values are given as means (n=3). [B] Western blot analysis with α-TcdE confirmed IPTG-induced expression of wildtype TcdE, TcdEΔN and TcdENC, respectively, after 1 h. The respective molecular weights are indicated. Evidence of TcdEΔNΔC expression was missing since TcdE antibody was directed towards the C-terminus.

4.1.3 The ratio of full length to truncated TcdE is regulated by a dual start motif

Many holins exhibit two start codons separated by one amino acid residue resulting in the expression of two proteins with different length and opposing function, acting as either a holin or as its inhibitor. The *tcdE* gene exhibits two additional start codons contributing to amino acids 25 and 27. Interestingly, DNA sequence analysis also indicated an alternative ribosome binding site (Shine-Dalgarno sequence AGGAGGC) upstream of the second and third start codons (Dove *et al.*, 1990). The deduced molecular weights of the proteins initiating from the first and from the third start codon are 19 kDa and 16 kDa, respectively.

To investigate the putative dual start motif site-directed mutagenesis was performed to generate point mutations within the Shine-Dalgarno sequence (SD I and SD II) or the start codons itself (Met), respectively.
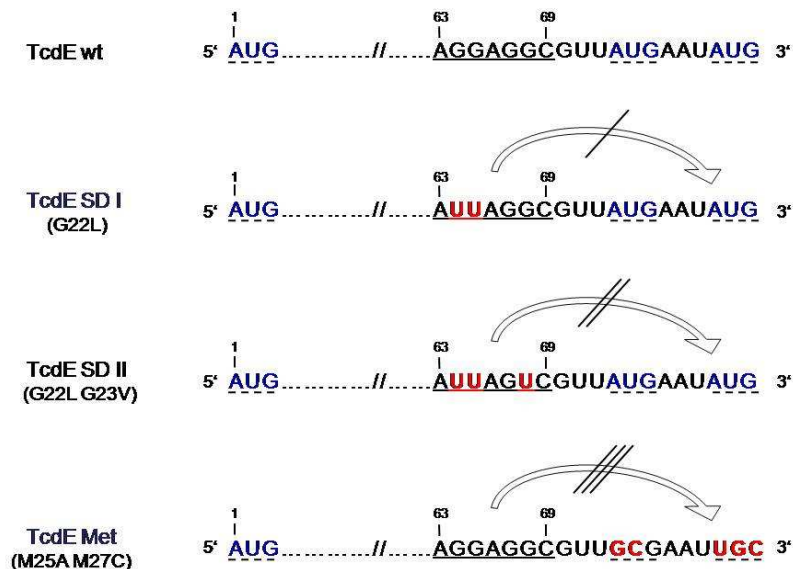
Fig. 4.5: Investigation of a putative dual start motif by using TcdE mutants. The N-terminal part of TcdE mRNA reflects three start codons AUG (blue, dashed) and a putative Shine-Dalgarno sequence (black, underlined) enabling the expression of protein of different length. Site-directed mutagenesis was performed to generate mutations within the Shine-Dalgarno sequence and the start codons, respectively (red). The Shine-Dalgarno mutants exhibit two (SD I) or rather three (SD II) point mutations reducing translation initiation at the following two start condons. The Methionine-mutant (Met) exhibiting point mutations in both start codons was generated to completely prevent translation initiation at the 2. and 3. start codons leading to full length TcdE, exclusively. The numbers above the mRNA sequence express the respective base pairs (bp).

Wildtype TcdE and the mutants were expressed in *E. coli* and Western blot analysis with specific anti-TcdE serum was performed showing strong expression already 0.5 h upon induction. The expression pattern of wildtype TcdE reflected a full length 19 kDa and an N-terminal shortened 16 kDa protein (Fig. 4.6, 1st panel). This observation was in accordance

with the deduced molecular weights of the proteins initiating from the first and the third start codons, respectively. Sequential mutation of base pairs within the putative Shine-Dalgarno sequence (Fig. 4.5, TcdE G22L [SD I] and TcdE G22LG23V [SD II]) shifted the ratio of full-length (19 kDa) to truncated (16 kDa) TcdE from 1 : 9 to approximately 4 : 6 (Fig. 4.6). This observation was a result of a reduced translation initiation at the third start codon confirming the existence of a functional dual start motif with respect to TcdE. Regarding the expression levels, wildtype TcdE can be considered as truncated 16 kDa TcdE. The Methionine-mutant (Fig. 4.5, TcdE M25AM27C [Met]) exhibits point mutations within the 2. and 3. start codons which completely prevented translation initiation leading to 19 kDa full length TcdE, exclusively (Fig. 4.6).
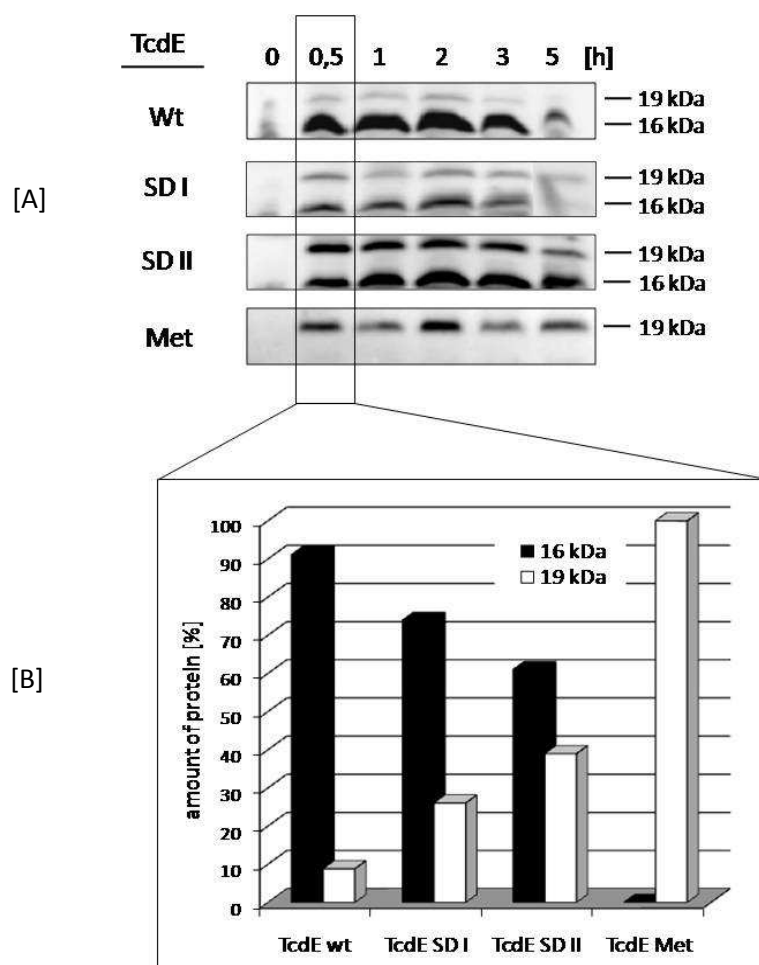
Fig. 4.6: The ratio of full length to truncated TcdE is regulated by a dual start motif. [A] Western Blot analysis with α–TcdE confirmed expression of full length TcdE and the respective mutants. The expression pattern of *E. coli* transformed either with full length TcdE or with the Shine-Dalgarno mutants (SD I, SD II) exhibited a 19 kDa and a 16 kDa protein. Expression of the Methionine-mutant reflected the full length TcdE, exclusively. [B] Densitometric analysis of protein expression after 0,5 h revealed a shift of the ratio of truncated (16 kDa, black bars) to full length TcdE (19 kDa, white bars) from 10 : 1 to approximately 1.5 : 1 following sequential mutation of base pairs within the Shine-Dalgarno sequence.

The growth profiles of *E. coli* expressing TcdE and the Shine-Dalgarno mutants SD I and SD II (Fig. 4.7) showed a strong decrease of the OD_{600} from 0.6 to 0.2 within 2 hours. Interestingly, this phenomenon was independent on the ratio of full length to truncated TcdE since bacteriolysis induced by wildtype TcdE as well as by SD I and SD II acted on the same kinetic. In contrast, expression of exclusively the full length TcdE (TcdE Met) resulted in bacteriostasis since bacterial growth stagnated 2 hours following induction.
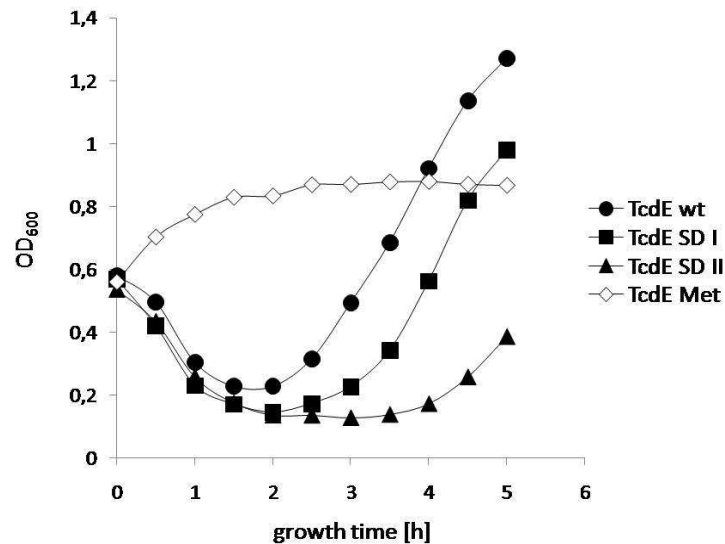
Fig. 4.7: Expression of wildtype TcdE and mutant TcdE in *E. coli*. The expression of full length TcdE (filled circles) and the Shine-Dalgarno mutants (SD I: filled squares, SD II: filled triangle) in *E. coli* resulted in a sudden loss of culture turbidity reflecting lysis of bacteria. The Met-mutant (open diamonds) induced bacteriostasis but not lysis. The recovery of the curves after 2 h concerning wildtype TcdE and SD-mutants is based on base insertions into TcdE DNA preventing expression of the active holin-like protein. In the case of the Met-mutant growth inhibitory of bacteria remains unaffected.

The different behavior of wildtype TcdE and the Methionine-mutant with regarding growth inhibition or lysis of bacteria were investigated by the ATP release assay. Thus, ATP release from *E. coli* expressing wildtype TcdE or the Met-mutant was measured 3 hours after induction. The Methionine-mutant, reflecting the 19 kDa full length TcdE, induced marginal ATP release compared to the vector control. Wildtype TcdE, which can be equated with truncated TcdE with respect to the expression pattern, induced a threefold higher ATP release confirming the bacteriolytic properties of the truncated TcdE compared to the full length protein.

Fig. 4.8: Truncated TcdE but not full length TcdE induces bacteriolysis. Supernatants of *E. coli* expressing wildtype TcdE or the Methionine-mutant for 3 hours were subjected to ATP determination assay. Wildtype TcdE, due to expression of full length and truncated TcdE, induced a threefold higher ATP release (19550 ± 1900) than TcdE-Met expressing only full length T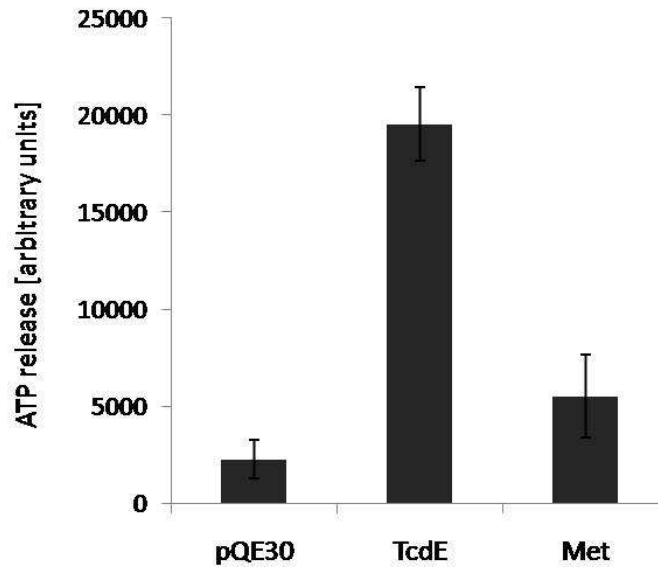cdE. The Methionine-mutant caused a slight effect (5500 ± 103) compared to the vector control (2300 ± 985). Values are given as means ± standard deviation in arbitrary units.

Regarding the growth profiles in Fig. 4.7 two hours after induction recovery of OD_{600} was observed. Unlike lysis, kinetic of recovery was different for wildtype TcdE and the respective mutants and thus, depended on the ratio of the full length to the truncated TcdE. While the optical density of *E. coli* expressing more than 90 % truncated TcdE (TcdE wt) started to recover after 2 hours, OD_{600}-recovery of *E. coli* expressing only 60 % truncated and 40 % full length TcdE (TcdE SD II) showed a 2 hours delay. 24 hours following induction OD_{600} of *E. coli* expressing TcdE wt and SD I and SD II reached a same value of almost 3.0 whereas *E. coli* transformed with TcdE-Met showed only a slight increase up to an optical density of 1.5.

DNA sequencing of single colonies expressing the different forms of TcdE excluded that this phenomenon was due to a loss of the plasmid harboring the *tcdE* construct. Rather, this observation was attributed to be based on base insertions into *tcdE* DNA accompanied by a disruption of the *tcdE* gene (Diploma thesis, S. Seehase). Western blot analysis displaying the protein levels in a time dependent manner confirmed the abortion of TcdE expression 5 hours following induction. After 24 hours TcdE almost completely disappeared. This phenomenon was observed in *E. coli* expressing wildtype TcdE as well as the mutants SD II and Met and was obtained for the full length and the truncated protein.
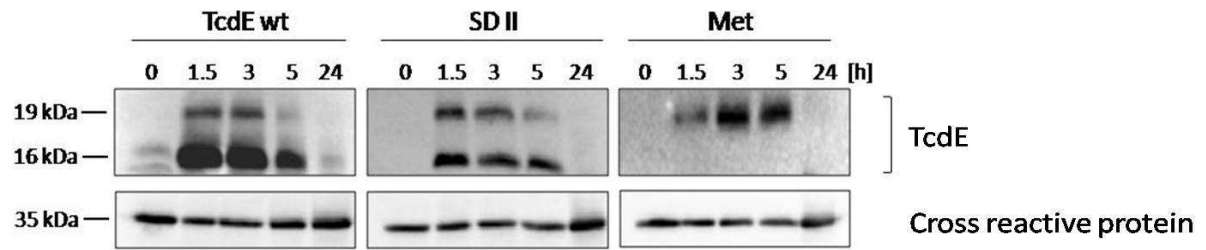
Fig. 4.9: TcdE- expression is aborted in a time-dependent manner. *E. coli* lysates expressing wildtype TcdE and the respective mutants (SD I and SD II, Met) were analyzed by Western blot using α–TcdE antiserum. A time-dependent abortion in expression of the full length and the truncated TcdE was observed for wildtype TcdE and the mutants SD II and Met. Cross reactive protein (35 kDa) was used as loading control and to exclude general protein degradation.

4.2 Investigation of a putative pathogenic role of *Clostridium difficile* TcdE

4.2.1 TcdE does not induce cytochrome *c* release from isolated mitochondria

It is still not clear whether *C. difficile* TcdE functions as a regulatory protein, a colonization factor or as a virulence factor. To investigate possible pathogenic properties isolated mitochondria of Hep2 cells were exposed to recombinant TcdE. As quantity for mitochondria disruption cytochrome *c* release was determined on the basis of Western blot analysis.
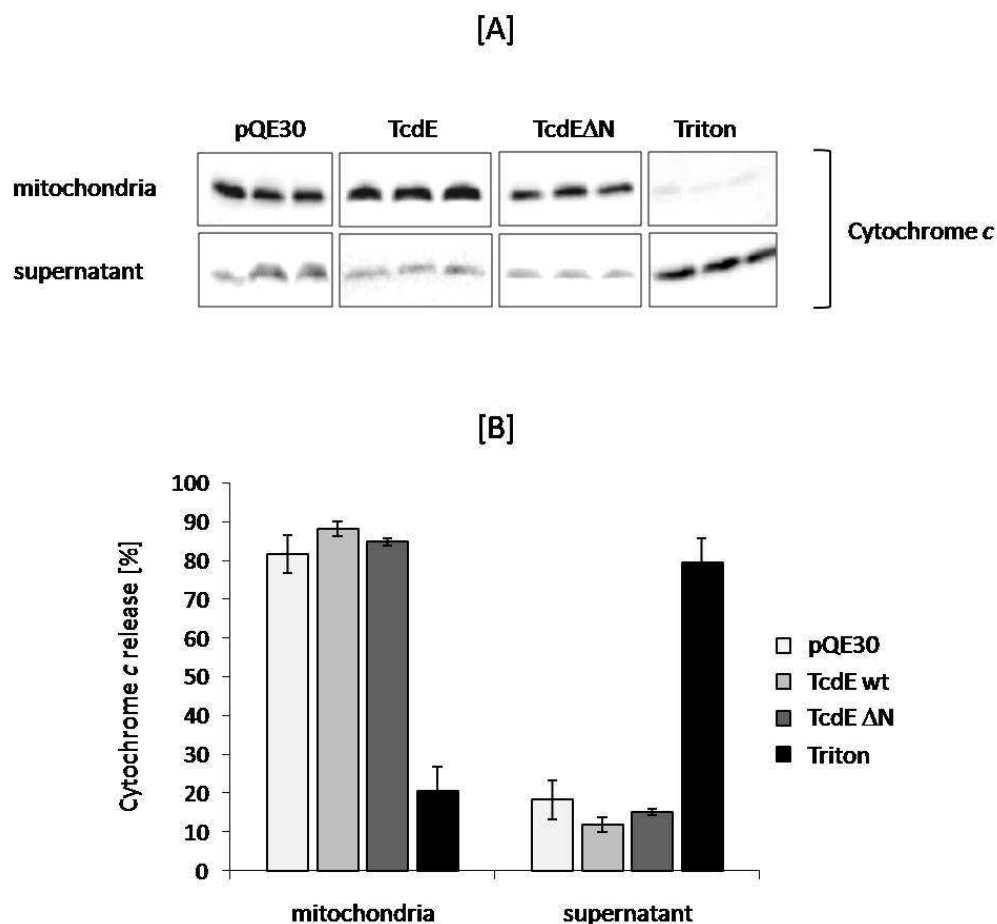
Fig. 4.10: TcdE did not induce cytochrome *c* release from isolated mitochondria. Isolated mitochondria of Hep2 cells were exposed to recombinant wildtype TcdE, exhibiting full length and truncated TcdE in a ratio 1 : 10, and the respective N-terminal shortened form TcdEΔN. [A] On the basis of Western blot analysis cytochrome *c* release was checked. [B] Densitometric evaluation of Western blot analyses. Cytochrome *c* release induced by wildtype TcdE and TcdEΔN was 11 % ± 1.9 % respectively 15 % ± 0.8 %. These values did not exceed background level (18 % ± 7 %) as indicated by the vector control. Triton X-100 served as positive control and induced cytochrome *c* release of 80 % ± 6 %. Values are given as means ± standard deviation (n=3).

As shown in Fig. 4.10, neither wildtype TcdE, reflecting the full length and the truncated protein products in a ratio 1 : 10, nor the N-terminal shortened form TcdEΔN induced cytochrom *c* release from mitochondria compared to the vector control. Background cytochrome *c* release of 11 % to 18 % was detected. Triton X-100 was used as positive control leading to 80 % ± 6 % of Cytochrome *c* in the supernatant. The data clearly show that TcdE did not induce mitochondria disruption.

4.2.2 TcdE does not induce apoptosis in Hep2 cells

To investigate a potential apoptotic effect Hep2 cells were transfected with the long and short TcdE. Cell morphology, actin cytoskeleton and activation of caspases-3 were examined by immunofluorescent staining. Transfection was performed with constructs harboring the full length *tcdE* gene or the N-terminal deleted gene *tcdEΔN*. In contrast to TcdE expression in bacteria, the eukaryotic expression system ensured production of exclusively full length TcdE when transfected with the full length construct since the eukaryotic translation apparatus does not utilize the prokaryotic alternative ribosome binding site. Thus, the system allowed distinguishing between full length and short TcdE.

As shown by myc immunostaining, full length TcdE as well as the N-terminal shortened bacteriolytic product was distributed within the cytoplasm concentrated around the nucleus (Fig. 4.11 [A]+[B]). Interestingly, presence of TcdE protein within the cytoplasmic membrane was excluded as pointed out by merging the pictures of myc and phalloidin staining (Fig. 4.11 [A]). Two different types of protein distribution within the cell were monitored: TcdE and TcdEΔN accumulated in the cytoplasm in terms of 'spots' with dense areas around the nucleus (Fig. 4.11 [C], left panel). On the other hand, interweaved, "maze-like" structures also concentrated in the neighborhood of the nucleus became visible (Fig. 4.11 [C], right panel). The two types were observed following 24h and 48h expression of both, full length TcdE and the N-terminal deleted product TcdEΔN (only shown for full length TcdE). The expression of each form didn't alter cell morphology nor induce fragmentation of DAPI stained nuclei after 24 h and 48 h (Fig. 4.11 [A], only shown for 48 h) indicating that TcdE does not affect viability of eukaryotic cells. Immunostaining against activated caspases-3 as an apoptotic marker confirmed this result since neither TcdE nor TcdEΔN activated caspase-3 after 48 h expression. Staurosporin treated cells served as positive control for staining of activated caspase-3 (Fig. 4.11 [B]). The absence of an alteration of nucleus and cell morphology and of activated caspases speaks against the hypothesis of TcdE acting as pathogenic factor.

[A]

Phalloidin	DAPI	Myc	Merge

pcDNA3.1

TcdE

TcdEΔN

[B]

Activated caspase-3	DAPI	Myc

Stauro

TcdE

TcdEΔN

[C]

Myc
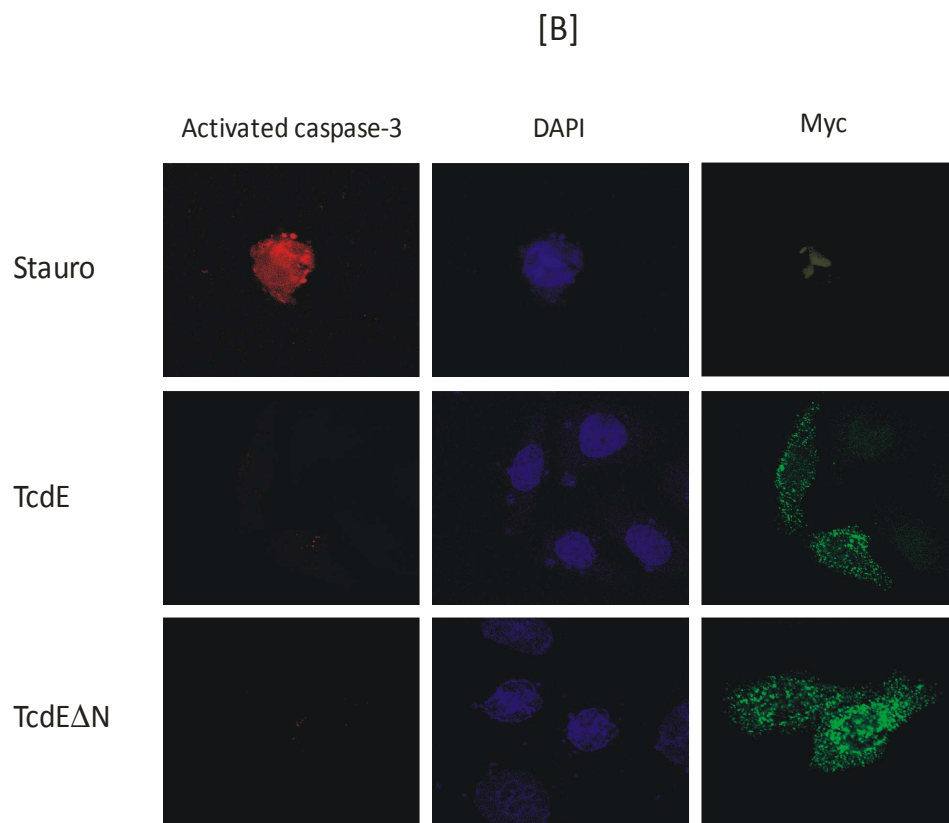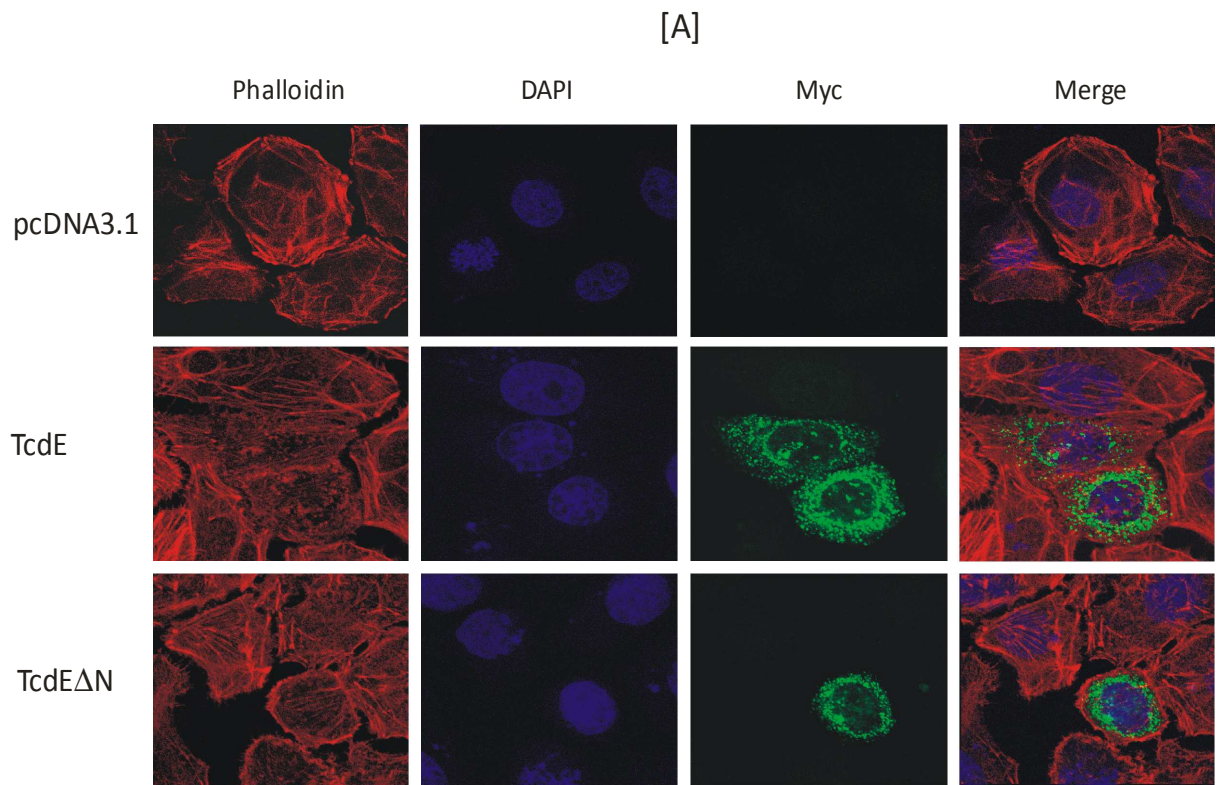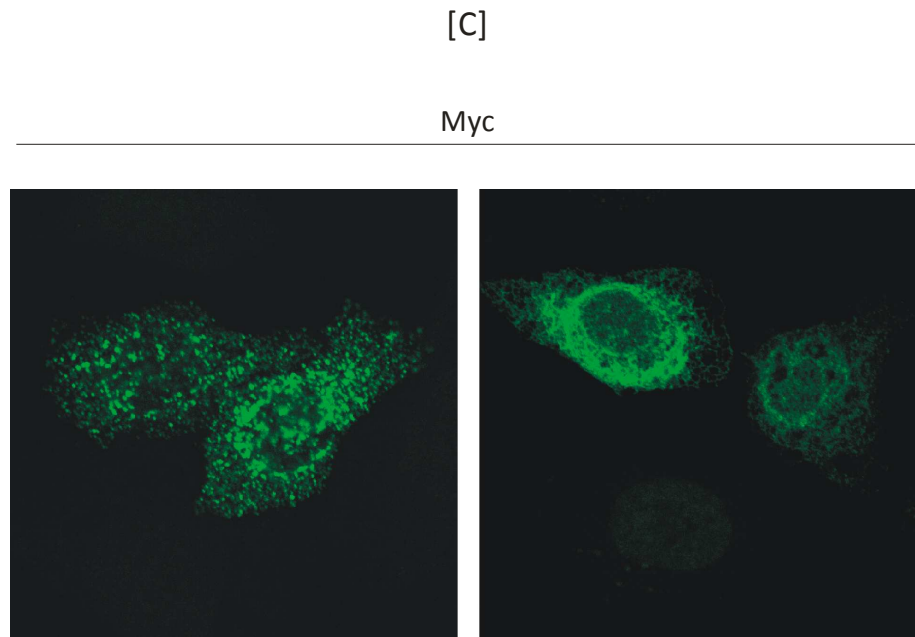
Fig. 4.11: TcdE is not involved in apoptosis. Hep2 cells grown on coverslips were transfected with full length TcdE, the N-terminal deletion mutant TcdEΔN or the empty vector pcDNA3.1. 24 h and 48 h following transfection immunofluorescence staining was performed (only shown for 48h). [A] Positive transfected cells are shown by α-myc immunofluorescence staining. Neither expression of full length TcdE nor TcdEΔN affected the nuclei or cell morphology as shown by DAPI staining and rhodamin-phalloidin staining of the actin cytoskeleton. [B] Additionally, staining against activated caspases-3 was performed. Neither TcdE nor TcdEΔN activated the apoptotic marker caspases-3. [C] Two different types of TcdE protein distribution were observed: protein accumulation forming "spots" (left panel) and interweaved "maze-like" structures (right panel).

4.3 *Clostridium difficile* specific characteristics

4.3.1 Toxin expression by *C. difficile* strains VPI10463 and 196

The hypothesis of TcdE to function as a release-factor for the pathogenic toxins TcdA and TcdB assumes a simultaneous expression of the three proteins. Western blot analysis displayed the protein levels of the pathogenic *C. difficile* strain VPI10463 and the hypervirulent PCR-ribotype 027 strain 196 in a time-dependent manner (Fig. 4.12 [A]). Densitometric evaluation of Western blot analysis of the reference strain cdi VPI10463 was performed to contrast TcdE expression with the appearance of TcdA and TcdB.
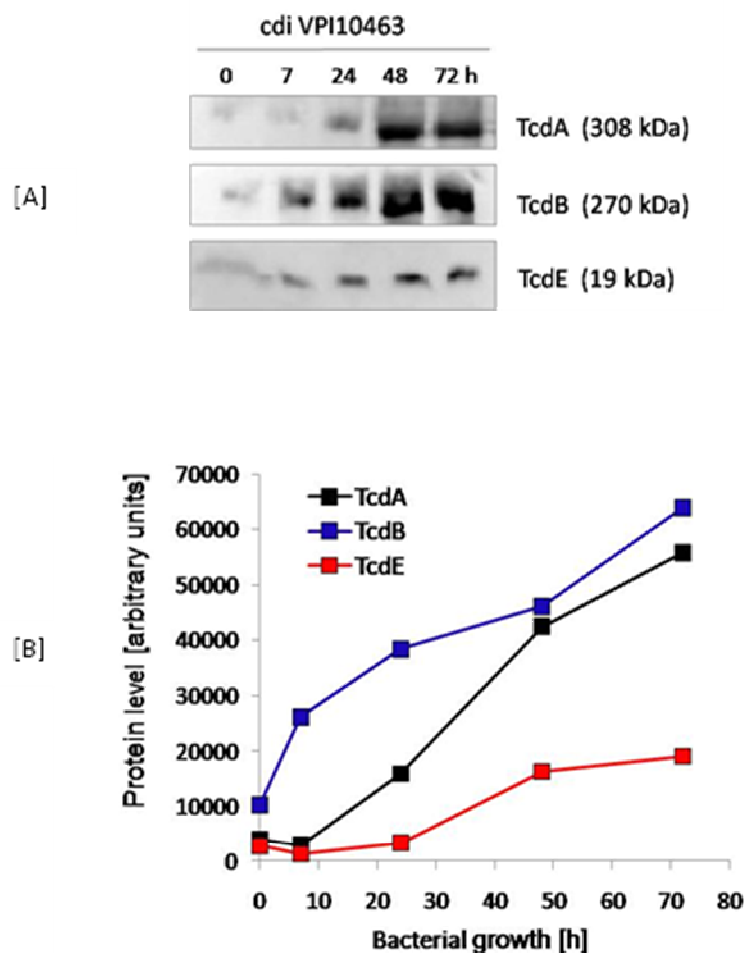
Fig. 4.12: **TcdE expression correlated with the appearance of the pathogenic toxins TcdA and TcdB.** [A] The pathogenic *C. difficile* strain VPI10463 was cultured for 72 h and samples were taken at indicated time points. The membrane fractions were lysed and subjected to Western blot analysis to detect TcdE levels. Interestingly, exclusively the full length TcdE was expressed. The proteins of the respective supernatants were precipitated and Western blot analysis with specific TcdA or TcdB antibodies was performed. [B] Densitometric analysis of toxin expression of cdiVPI10463 revealed a temporal correlation between TcdE expression and the appearance of the toxins TcdA and TcdB. Protein levels are given in arbitrary units.

TcdE was expressed already after 7 h of cultivation. Levels increased up to 48 h reaching a plateau phase. Since the appearance of TcdE in the membrane fraction and accumulation of the respective glucosyltransferases TcdA and TcdB in the supernatant occurred simultaneously, the hypothesis of TcdE facilitating the release of the pathogenic toxins to the extracellular environment was supported.

Interestingly, in difference to TcdE expression in *E. coli* exclusively the 19 kDa full length TcdE was detected in *C. difficile*.

An interesting observation was the transient increase of the bacterial cell population with a maximum of OD_{600} at approximately 25 hours. The following reduction in the optical density to a value of 1 was accompanied by a considerable 4-fold increase in toxin expression, exemplified for TcdA. Hence, cell count and release of the pathogenic toxins TcdA/B correlated vice versa.
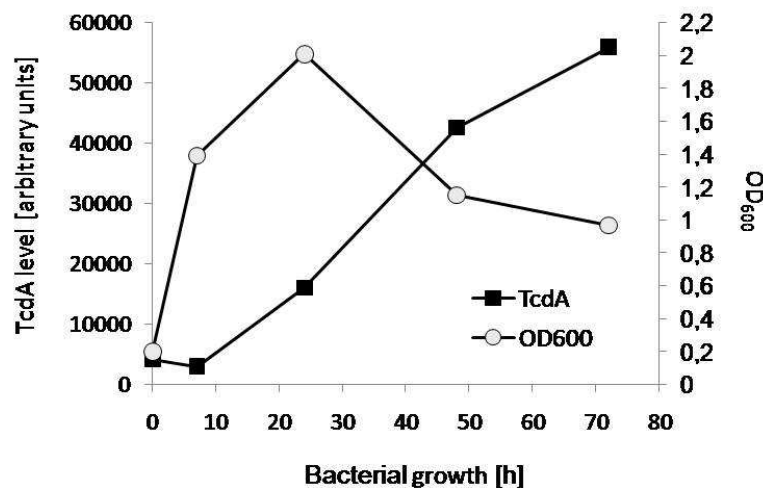
Fig. 4.13: TcdA expression correlated vice versa with bacterial cell count. TcdA levels (black squares) are mapped towards the OD_{600} (grey circles) at the respective time points. A strong increase in bacteria count was accompanied by a slight TcdA expression. Following maximum in cell density the OD_{600} was reduced from 2 to 1 while the TcdA level increased 4-fold. TcdA levels, as analyzed by densitometrical evaluation of Western blot analysis, are given in arbitrary units.

4.3.2 Sporulation of low and high toxin producing *C. difficile* strains

Sporulation is one of the main characteristics of clostridia and of ecological advantage to the organism as it enables to survive under adverse conditions. Thus, sporulation occurs under condition of nutrient depletion which is present after long time culturing. To investigate whether TcdE is involved in *C. difficile* sporulation, TcdE expression and sporulation rates of different *C. difficile* strains were compared. Hence, Gram stain of liquid culture was used to visualize and examine sporulation. Fig. 4.14 illustrates the development of Gram positive

rods from 8 h to 72 h of cultivation exemplified for the hypervirulent *C. difficile* strain 196. During the logarithmic growth phase exclusively vegetative bacteria were observed characterized by a homogeneous distribution of the cristal violet stain (8 h). After 48 h of cultivation endospores became visible that developed within the rod and escaped the Gram stain. Time dependently, most of bacterial cells appeared Gram negative which was due to reconstruction processes inside the cell wall known for older Gram positive bacteria.

8 h   48 h   72 h
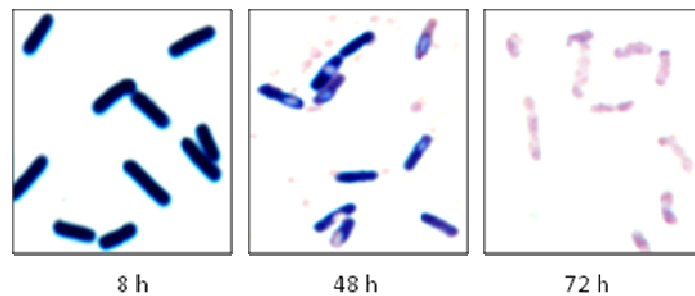
Fig. 4.14: Gram stain of *C. difficile* strain 196. At indicated time points samples of *C. difficile* liquid culture were taken and subjected to Gram staining. Time dependently, Gram positive rods became Gram negative due to reconstruction processes inside the cell wall. Furthermore, *C. difficile* formed endospores with one spore per cell displayed after 48 h of culturing.

Sporulation rates of the *C. difficile* reference strain VPI10463, the variant strain 1470 serotype F and the hypervirulent strain 196 (PCR ribotype 027) were compared.
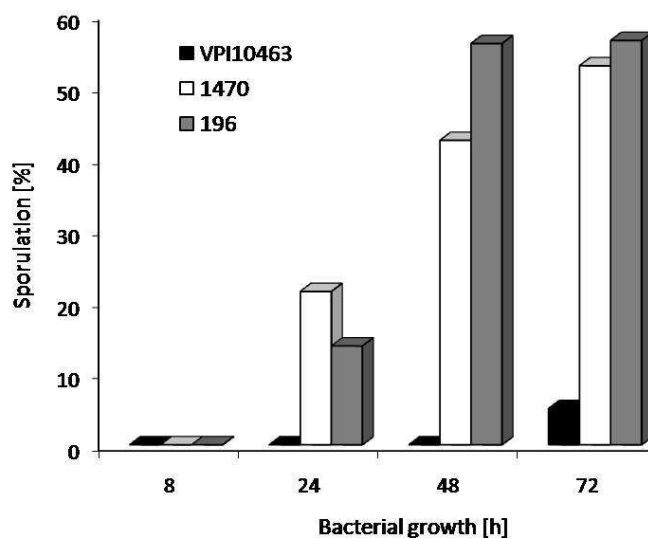
Fig. 4.15: Comparative analysis of sporulation of *C. difficile* strains VPI10463, 1470 and 196. Samples of liquid cultures of the different strains at the respective time points were subjected to Gram staining to visualize spore formation. The high toxin producing strain VPI10463 showed a low sporulation rate of 5 % after 72 h. In contrast the hypervirulent strain 196 and the variant strain 1470 started sporulation at earlier time points (24 h) and with higher values of almost 60 % after 72 h. Sporulation was quantitated as endospores per total bacterial cells and given in %.

Therefore, Gram stainings of the respective samples were performed and sporulation was quantified. As shown in Fig. 4.15 the high producer strain *C. dificile* VPI10463 exhibited a low sporulation efficacy of 5 % spores per total cells not until 72 h of cultivating. In contrast, 15 % of bacteria of the hypervirulent strain *C. difficile* 196 formed endospores already after 24 h and almost 60 % after 48 h. The results of the strain *C. difficile* 1470 serotype F were comparable to the hypervirulent strain and exhibited 60 % sporulation after 7 h. Thus, the toxin high producing *C. difficile* strain VPI10463 exhibited a more than 10- fold less sporulation efficacy than the hypervirulent strain 196 and the variant strain 1470 serotype F.

4.3.3 Comparative analysis of TcdE expression in low and high sporulating *C. difficile* strains

To investigate whether TcdE is involved in the difference of the sporulation efficiencies between the hypervirulent 196 and the reference strain VPI10463 TcdE expression levels were determined. Therefore, lysates of clostridia were prepared at the indicated time points and Western blot analysis with polyclonal anti-TcdE antibody was performed.
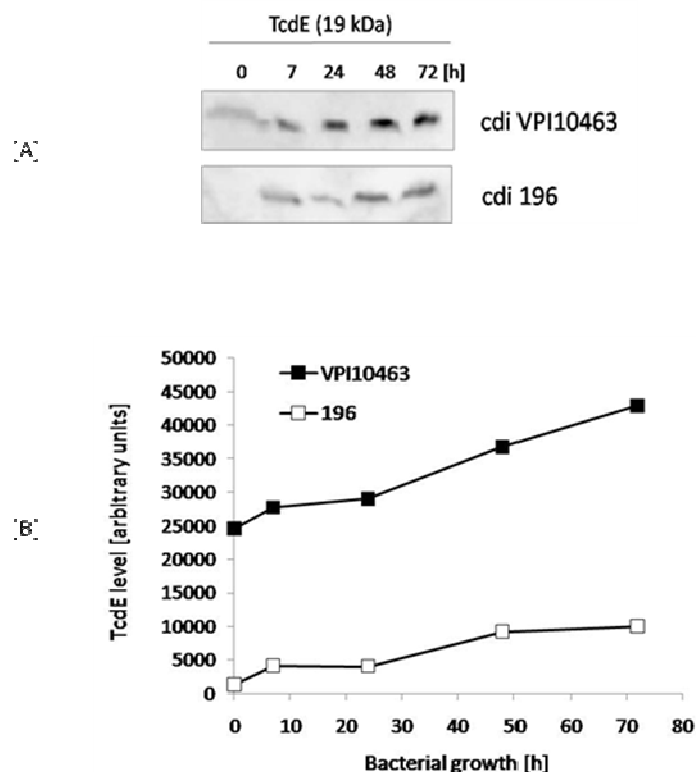
Fig. 4.16: Comparative analysis of TcdE expression in the reference strain *C. difficile* VPI10463 and the high sporulating hypervirulent strain *C. difficile* 196. [A] Western blot analysis of clostridia lysates with α-TcdE was performed to compare the TcdE levels in *C. difficile* strains VPI10463 and 196 in a time dependent manner. Therefore lysates were adjusted to bacterial cell count. [B] Densitometric analysis revealed an almost 5-fold excess of TcdE expression in reference strain VPI10463 (black squares) compared to the hypervirulent, high sporulating strain 196 (white squares). TcdE levels are given in arbitrary units.

The volume subjected to SDS-PAGE was adjusted to bacterial cell count allowing direct comparison of the immunoblots. Interestingly, among sporulation efficacies also TcdE levels differed in the reference strain VPI10463 compared to the hypervirulent strain 196. Densitometric analysis revealed an almost 5- fold excess of TcdE expression in the reference strain VPI10463 compared to the high sporulating *C. difficile* strain 196.

4.4 Investigation of TcdE function via specific insertional inactivation of *tcdE* in *Clostridium difficile* strain 630Δ*erm*

4.4.1 Insertional inactivation of *tcdE* using the ClosTron method

Splicing by Overlap Extension PCR (SOE PCR) was performed to amplify a 353 bp product containing the modified IBS, EBS1d and EBS2 sequences which are specific for the target gene *tcdE* and responsible for intron targeting (Fig. 4.17 [A]). The following HindIII and BsrGI digests prepared the PCR product for ligation into digested and purified plasmid pMTL007C-E2. An insertion of the 350 bp product into plasmid pMTL007C-E2 can be checked by PCR. A 560 bp band reflected positive ligation compared to a 440 bp band amplified from the digested plasmid alone (Fig. 4.17 [B]). Finally, construct pMTL007C-E2: Cdi-*tcdE*-234a was sequenced to verify correct insertion.
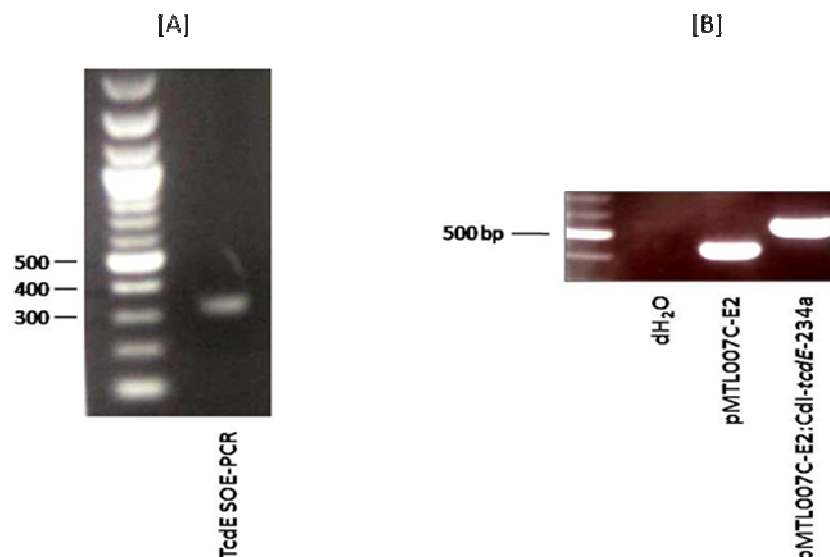
Fig. 4.17: Generation of construct pMTL007C-E2: Cdi-*tcdE*-234a. [A] One-tube SOE-PCR (**S**plicing by **O**verlap **E**xtension) was performed to amplify a 353 bp product containing the modified IBS, EBS1d and EBS2 which are responsible for intron targeting. HindIII and BsrGI restriction sites were generated followed by a purification step to prepare the insert for ligation. Agarose gel electrophoresis (1%) was used as detection method visualizing a specific 350 bp band. [B] Digested and purificated PCR-product was ligated over night at 16°C in plasmid pMTL007C-E2 which offers also the HindIII and BsrGI restriction sites. Positive ligation was checked by PCR followed by agarose gel electrophoresis (1 %). Correct insertion resulted in a 440 bp PCR product compared to the negative control pMTL007C-E2 with a 560 bp PCR product.

Subsequent to transformation of *E. coli* donor CA434 with construct pMTL007C-E2: Cdi-*tcdE*-234a, conjugation with the recipient *C. difficile* 630Δ*erm* was performed. Afterwards, transconjugants were selected by antibiotics using erythromycin resistance which was acquired by intron insertion. Genomic DNA of selected transconjugants was isolated and PCR screening was performed to identify the desired knockout. Amplification of the intron-exon junction gave unambiguous information. As shown by agarose gel electrophoresis, the expected 449 bp PCR product was amplified in 16 out of 17 clones. Plasmid pMTL007C-E2 and genomic DNA from the initial strain cdi630Δ*erm* were used as negative controls. Finally, correct insertion was additionally ensured by sequencing.

Fig. 4.18: PCR screening for gene knockout. PCR screening and following sequencing was used to unambiguously identify the desired insertional inactivation of the *tcdE* gene. An intron universal primer and a specific *tcdE* primer were used to amplify the intron-exon junction. An agarose gel (1%) displayed a 449 bp PCR product confirming intron insertion into the expected *tcdE* targeting region.

4.4.2 Evidence of insertional inactivation of *tcdE* on protein level

DNA-sequencing evidenced the successful insertional inactivation of the *tcdE* gene in *C. difficile* strain 630Δ*erm*. Additionally, Western blot analysis was performed to confirm TcdE- knockout on protein level. Therefore, lysates of cdi630Δ*erm* and cdi630Δ*tcdE* were prepared after 24 h cultivation and the insoluble fraction was subjected to SDS-PAGE. Western blot analysis with TcdE antibody revealed strong expression of a 19 kDa protein in the reference strain cdi630Δ*erm* which was not observed in the TcdE- knockout strain cdi630Δ*tcdE*.
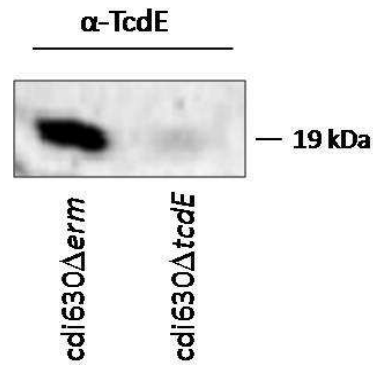
Fig. 4.19: Evidence of insertional inactivation of *tcdE* on protein level. Lysates of cdi630Δ*erm* and cdi630Δ*tcdE* after 24 h cultivation were prepared by means of mechanical cell disruption using the French Press. The insoluble membrane fraction was separated from the soluble fraction and resuspended in detergent containing buffer. Following incubation for 30 min at 4°C the suspension was subjected to SDS-PAGE and Western blot analysis with α-TcdE. The reference strain cdi630Δ*erm* obtained a strong expression of a 19 kDa protein which was not observed in the TcdE- knockout strain cdi630Δ*tcdE*.

4.4.3 Release of the pathogenic toxins TcdA and TcdB from mutant strain cdi630Δ*tcdE*

TcdE is supposed to participate in the release of the pathogenic toxins TcdA and TcdB. To investigate this hypothesis toxin release from *C. difficile* 630Δ*erm* and the TcdE- knockout strain cdi630Δ*tcdE* was compared. Therefore, supernatants of both strains were collected at indicated time points and precipitated proteins were subjected to SDS-PAGE and Western blot analysis with specific TcdA and TcdB antibodies. As shown in Fig. 4.20, Western blots reflected comparable toxin levels released from cdi630Δ*erm* and cdi630Δ*tcdE* with a slight increase regarding the mutant strain.
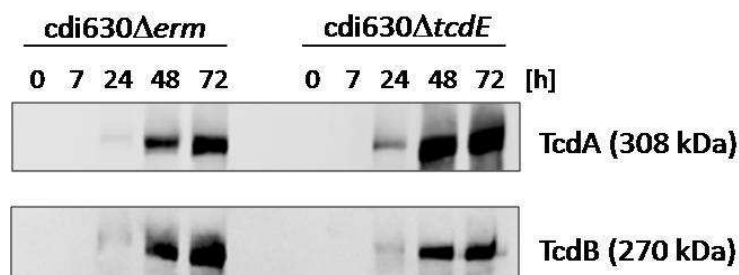
Fig. 4.20: Release of TcdA and TcdB from *C. difficile* strain 630Δ*erm* and the TcdE-knockout strain cdi630Δ*tcdE*. Supernatants of *C. difficile* strains cdi630Δ*erm* and cdi630Δ*tcdE* were collected at indicated time points and chloroform methanol precipitation was performed. Resuspended protein was subjected to SDS-PAGE (7.5 %) and Western blot analysis with specific TcdA and TcdB antibodies was performed. TcdE is not decisive involved in release of the pathogenic toxins since its knockout did not affect kinetic of toxin release nor absolute TcdA and TcdB levels.

In addition to the comparative analysis of the TcdA- and TcdB expression levels, functional assay was performed utilizing the toxin-induced cytopathic effect.

[A]

[B]
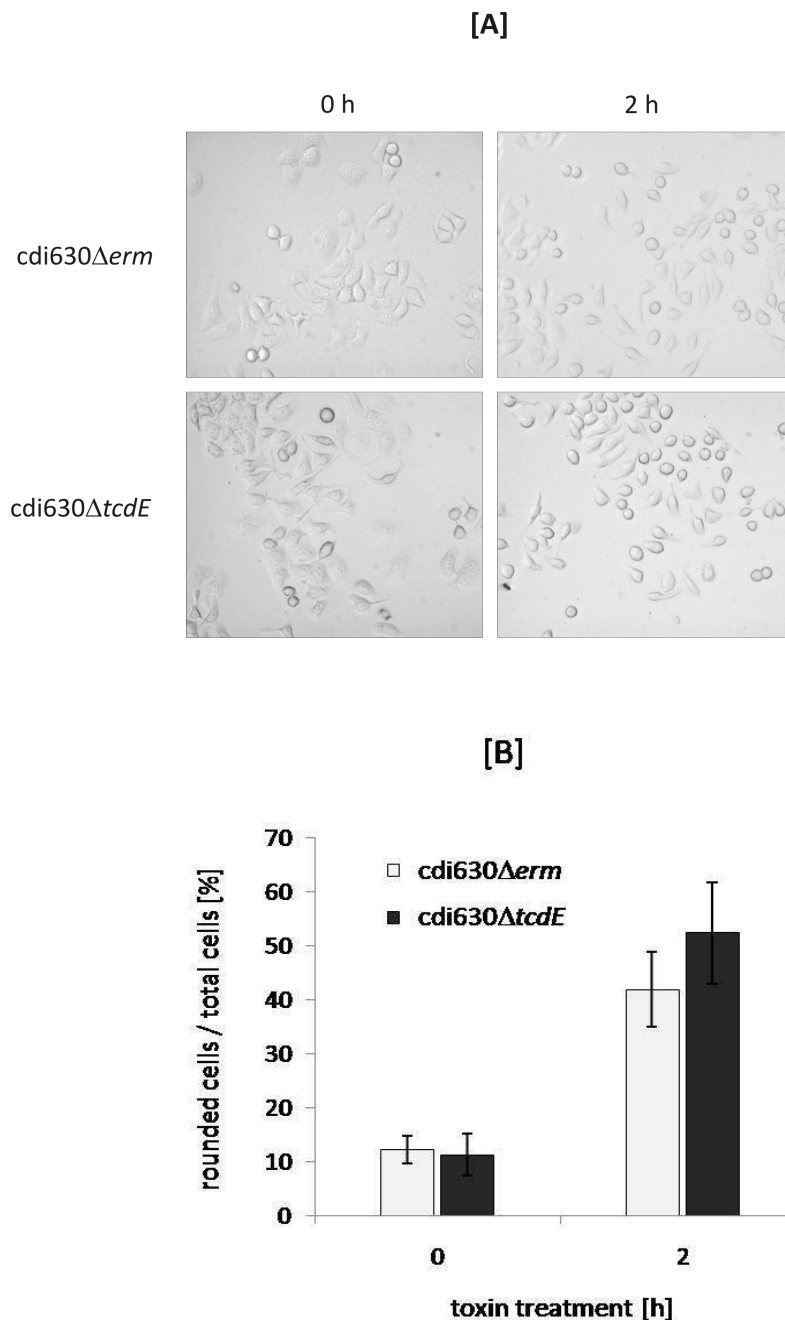
Fig. 4.21: Cytopathic effect of Hep2 cells induced by *C. difficile* strain 630Δ*erm* and the TcdE- knockout strain cdi630Δ*tcdE*. [A] Hep2 cells grown in 24 well chambers were exposed to 250 µl supernatants of cdi630Δ*erm* and cdi630Δ*tcdE* cultivated for 48 h. Cell rounding was recorded by means of light microscopy 0 h and 2 h after addition of toxins. [B] Cytopathic effect was quantified as rounded cells per total cells in %. Supernatants of cdi630Δ*erm* and cdi630Δ*tcdE* caused 42 % ± 7 %, respectively 52 % ± 9 % rounded cells per total cells after 2 h compared to basal levels of about 12 %. In consideration of the standard deviations, TcdA and TcdB levels released from the *C. difficile* strains cdi630Δ*erm* and cdi630Δ*tcdE* were comparable, although the TcdE- knockout strain showed a slight increase in toxin release. Values are given as means ± standard deviations (n = 10).

Therefore, Hep2 cells were exposed to supernatants of *C. difficile* strains cdi630Δ*erm* and cdi630Δ*tcdE* cultivated for 48 h. Cytopathic effect (cell rounding), which is based on disassembly of the actin cytoskeleton, was quantified 0 h and 2 h after addition of toxins as rounded cells per total cells (%). Cell morphology of Hep2 cells treated with supernatant of the reference strain cdi630Δ*erm* is exemplified in Fig. 4.21 [A] displaying toxin- induced cell rounding. Quantification is shown in Fig. 4.21 [B].

Basal levels of cell rounding subsequently upon exposure of the cells to the supernatants were about 12 %. Two hours after treatment, supernatants from reference strain cdi630Δ*erm* and mutant strain cdi630Δ*tcdE* caused cell rounding of 42 % ± 7 % respectively 52 % ± 9 %. In consideration of the standard deviations, these data support the results of Western blot analysis. TcdE- knockout strain cdi630Δ*tcdE* exhibited similar amounts of released TcdA and TcdB compared to the reference cdi630Δ*erm*. However, the TcdE-mutant strain showed a slight increase in toxin release.

Taken together, the data indicate no decisive involvement of TcdE in the release of the pathogenic toxins from *C. difficile* as it was suggested by Dove *et al*. (1990).

4.4.4 Comparative analysis of growth rates and sporulation efficacies of *C. difficile* strain 630Δ*erm* and the respective TcdE- knockout strain cdi630Δ*tcdE*

Growth and sporulation rates of *C. difficile* strain 630Δ*erm* and TcdE- knockout strain cdi630Δ*tcdE* were examined to investigate a possible correlation with TcdE expression. The results are illustrated in Fig. 4.22. The optical density (OD_{600}, filled squares) reflecting bacterial growth was determined in a time dependent manner. After 24 h of cultivation growth curves of cdi630Δ*erm* and cdi630Δ*tcdE* exhibited an OD_{600} maximum of almost 1.8. Following cultivation, optical densities decreased within 48 h to a constant value of 0.5. Interestingly, this reduction in cell count was accompanied by an increase in the sporulation rate (filled circles). While no sporulation occurred until 24 h, 18 % ± 4.5 % of bacteria of strain 630Δ*erm* (black circles) and 23 % ± 10 % of the strain cdi630Δ*tcdE* (red circles) formed endospores after 48 h. After 72 h of cultivation, sporulation of both strains resulted in the same value of approximately 25 %. Thus, the TcdE- knockout strain cdi630Δ*tcdE* possessed a marginal increased sporulation rate at 48 h compared to the respective reference strain cdi630Δ*erm*. Even under standardized conditions these results showed high standard deviations. This phenomenon might contribute to sensitive bacterial growth which depended on conditions as temperature, pH value, cell count et cetera.

In consideration of even high standard deviations TcdE did neither affect kinetic of sporulation nor absolute sporulation values. The reduction in cell count and an increase of sporulation was the only correlation that was observed in this study independently of TcdE expression.
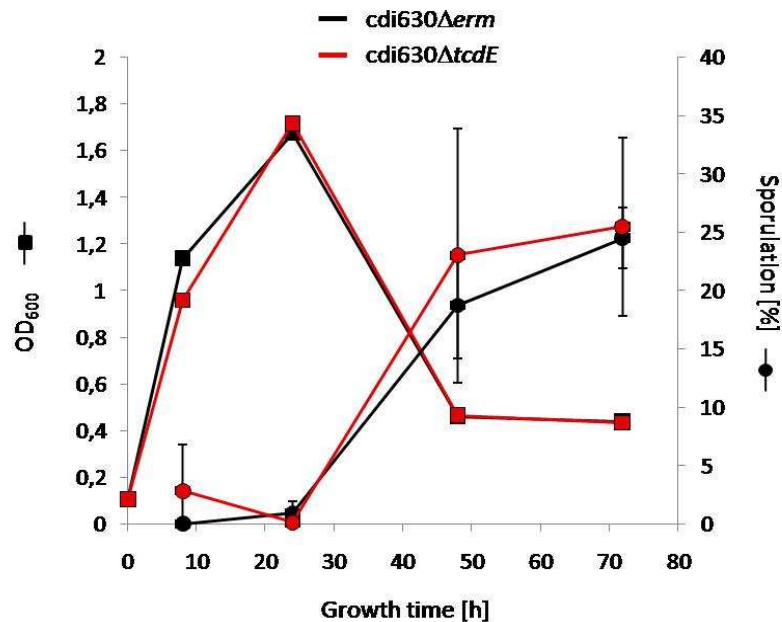
Fig. 4.22: Comparative analysis of growth rates and sporulation efficacies of *C. difficile* strain 630Δ*erm* and the respective TcdE- knockout strain cdi630Δ*tcdE*. Growth profiles of cdi630Δ*erm* and the mutant strain cdi630Δ*tcdE* developed congruently with an OD_{600} maximum of 1.8 at 24 h followed by a strong decrease to a constant value of 0.5 after 48 h and 72 h of cultivation. Interestingly, this rapid reduction in cell count was accompanied by an increase in sporulation to 18 % ± 4.5 % for cdi630Δ*erm* (red circles) and 23 % ± 10 % (black circles) for the respective TcdE- knockout strain cdi630Δ*tcdE*. Values are given as means ± standard deviation (n=10).

5. Discussion

5.1 Effect of *Clostridium difficile* TcdE on bacteria

The small open reading frame *tcdE* within the pathogenicity locus of *Clostridium difficile* encodes a 19 kDa, highly hydrophobic protein of unknown function. Since *C. difficile* resides in the colon, TcdE could be involved in virulence by affecting either intestinal commensals or the enterocytes. Otherwise, TcdE could have regulatory function with regard to expression or release of the toxins A and B. Previous studies revealed a correlation between TcdE expression and inhibition of bacterial growth, however, without detection in SDS-PAGE or immunoblot. Amino acid sequence analysis supported the idea of TcdE as bacteriolytic protein because of sequence and structural homologies to bacteriophage-encoded holins (Tan *et al*., 2001). The present study investigates different aspects of TcdE function including structure-function analysis, effects on *E. coli* and epithelial cells and involvement in specific features of *C. difficile* like sporulation, growth and toxin release. The analyzed putative functions of *C. difficile* TcdE are illustrated in the scheme below.
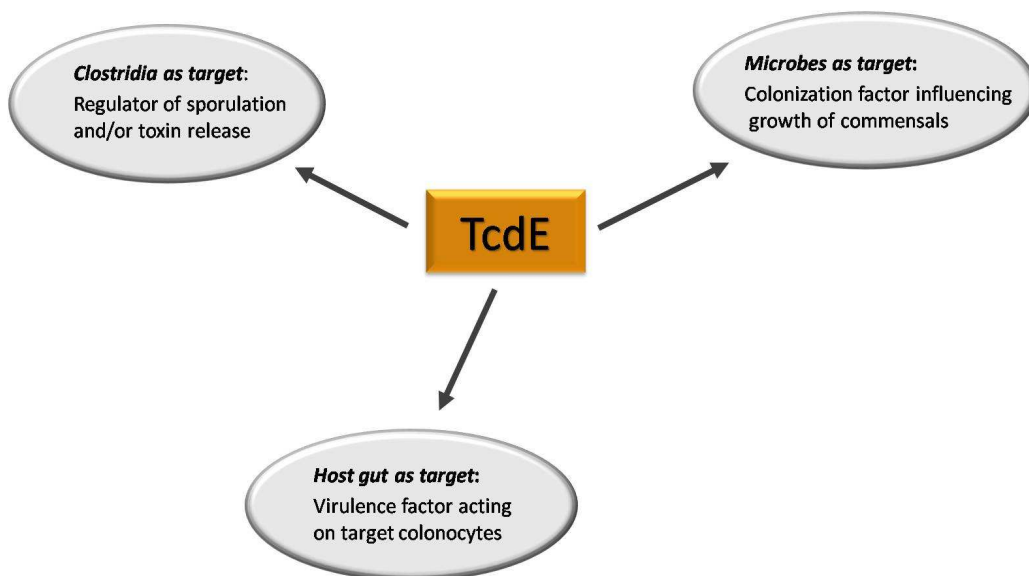
Fig. 5.1: Putative functions of *C. difficile* TcdE.

5.1.1 TcdE induces lysis of *E. coli*

T7 Express *lysY/I*^{q} competent *Escherichia coli* were used to investigate TcdE-induced inhibition of bacterial growth as they afford a tight expression control enabling cloning of toxic genes. Growth profiles of *E. coli* transformed with wildtype TcdE showed a strong loss of culture turbidity already 30 min after induction. This phenomenon was not observed in *E. coli* transformed with the empty vector (Fig. 4.1 [A]). Since TcdE shares sequence and structure homologies to bacteriophage-encoded lytic holins, decrease in optical density was supposed to be based on TcdE-induced bacteriolysis. This assumption was supported by ATP release from *E. coli* as marker for cell lysis. Tan and co-workers also showed gradual loss of culture turbidity after induction of *E. coli* transformed with a TcdE-construct, which was independent on media, *E. coli* strains and temperature. The hypothesis that the site of action of TcdE is at bacterial cell membranes was supported by Transmission electron microscopy confirming loss of membrane integrity and bacterial death as a result of membrane disruption (Tan *et al.*, 2001). However, the authors were unable to detect the protein TcdE by SDS-PAGE or immunoblot analysis and, thus, couldn't verify the causal correlation for TcdE-induced bacteriolysis.

The unsuccessful attempts to visualize TcdE by SDS-PAGE indicated that protein quantities below the SDS-PAGE resolution are sufficient for affecting cell growth. Therefore we generated a specific polyclonal rabbit antibody for detecting TcdE in a more sensitive Western blot. In fact we confirmed the expression of the predicted 19 kDa protein in *E. coli* finally adducing evidence for TcdE-mediated lysis of bacteria. Interestingly, an additional 16 kDa protein was detectable with a tenfold excess compared to the 19 kDa full length protein.

Furthermore, growth profiles of *E. coli* expressing TcdE showed a transient reduction in optical density. Two hours after induction minimal cell count was reached followed by a recovery of bacterial population. Also Goh and co-workers observed a biphasic growth profile of *E. coli* expressing TcdE without performing any further investigations or giving explanations. As the reversal in growth inhibition correlated with disappearance of TcdE protein after 3 h (Fig. 4.9) and a second IPTG induction after 24 h didn't induce inhibitory effects again (Seehase S.), DNA sequencing of single colonies was performed; the aim was to investigate molecular effects of TcdE expression on the bacterial genome. Sequence analyses excluded that this phenomenon was due to a loss of the plasmid harboring the *tcdE*-construct. Rather, base insertions of 700 bp to 1,000 bp into the *tcdE* gene were observed causing its disruption (Seehase S.). Hence, mutational inactivation can be construed as a bacterial regulation against TcdE-induced toxicity leading to a mixed population of *E. coli*. It has still to be clarified whether growth recovery 3 h after induction of TcdE expression is also due to a functional inactivation of the gene.

5.1.2 Role of the dual start motif and impact of TcdE domains

Many bacteriophage-encoded holins use a dual start motif to produce two proteins differing in length and function: the holin and its inhibitor the antiholin, which possess a Met-Lys extension in case of the λ-holin. Interestingly, analysis of the *tcdE* nucleic acid sequence revealed two additional ATG start codons contributing to amino acids 25 and 27. Additionally, an alternative Shine-Dalgarno sequence, which is part of the ribosome binding site, was found upstream of both the first (GGTGG) and third (GGAGG) start codons of *tcdE* (Dove *et al.*, 1990) indicating the existence of a functional dual start motif. The TcdE protein expression pattern supported the hypothesis since a 16 kDa protein was detected in addition to the 19 kDa full length TcdE (Fig. 4.1 [B]). This was in accordance with the deduced molecular weights of the proteins initiating from the second/third putative translation initiation sites (Tan *et al.*, 2001).

To investigate the putative dual start motif, TcdE mutants exhibiting point mutations within the Shine-Dalgarno sequence or the alternative ATG start codons (Fig. 4.5) were generated and expressed in *E. coli*. The expression pattern of wildtype TcdE revealed only 10 % of 19 kDa full length TcdE compared to about 90 % of truncated 16 kDa protein (Fig. 4.6 [A], 1st panel). As the antiserum recognizes the C-terminus of TcdE, truncation is very likely at the N-terminal part. Furthermore, protein detection correlated well with the respective growth profile of wildtype TcdE. Already 0.5 h after induction strong protein expression occurred correlating with a dramatic decrease in culture turbidity (Fig. 4.6 [A] and Fig. 4.7). Subsequently, protein levels remained constant up to 3 h post-induction followed by a consecutive disappearance of full length and truncated TcdE. Interestingly, protein abortion was associated with recovery of bacteria population. Unfortunately, the evidence of a mixed population of *E. coli* still expressing the lytic TcdE and those containing a disrupted or lost *tcdE* gene was observed for bacteria grown for 24 h. Thus, DNA insertion into the *tcdE* gene as bacterial counter-regulation against TcdE-induced toxicity might not explain the early reversal in growth inhibition.

The Shine-Dalgarno mutants SD I and SD II, exhibiting two or rather three point mutations within the Shine-Dalgarno sequence (Fig. 4.5), showed different expression pattern compared to wildtype TcdE. The ratio of full length (19 kDa) to truncated TcdE (16 kDa) shifted from 1 : 10 to about 1 : 1.5 for SD II confirming a reduced translation initiation from the third start codon as a result of ribosome binding site mutations and thus, the existence of a functional dual start motif. Interestingly, the shift of the ratio of full length to truncated TcdE altered kinetic of the recovery of the bacteria population. Wildtype TcdE, expressing only 10 % full length and 90 % short TcdE, showed the fastest reversal in growth inhibition after 2 h whereas *E. coli* producing full length and short TcdE in a ratio of 40 % to 60 % (SD II) recovered with a two hours delay (Fig. 4.6 and Fig. 4.7). The reversal in bacterial growth can be interpreted as a successful response to the strong selection force of bacteriolytic TcdE. This conclusion is supported by the Methionine-mutant, which exclusively expresses full length TcdE and indeed induces plateau of bacterial growth but not lysis.

While recovery time depended on the ratio of full length to truncated TcdE, kinetic of lysis was not altered since the growth curves regarding wildtype TcdE and the SD mutants developed congruently up to 2 h (Fig. 4.7). Thus, the presence of truncated TcdE per se is more important that the ratio to the full length protein.

It is known that the λ-holin S105 and the antiholin S107, which possesses a Lys-Met-extension, are produced during infection at a constant ratio of 2:1 (Bläsi and Young, 1996; Ryan and Rutenberg, 2007). It was suggested that the holin and antiholin molecules accumulate as a hetero-oligomeric patch at the inner membrane and rearrange in a second step to form a pore. This rearrangement is essential, but inhibited by the interaction of the amino-terminal positive charge (Lys) of the S107 molecules with the negatively charged inner surface of the energized membrane. As described in detail by Bläsi *et al.* (1990), S107 acts as lysis inhibitor as long as the membrane potential is maintained and it also contributes actively to pore formation when the membrane potential collapses. Thus, not only the two protein products S105 and S107 have opposing function but also the so called antiholin itself has dual capacity.

A similar process can be suggested for TcdE. Since TcdE mutant ΔNΔC, only consisting of the three transmembrane domains (TMDs), inhibited bacterial growth whereas a fusion construct of only the N- and C-termini didn't appreciably affect growth of bacteria, the three TMDs are shown to be essential for TcdE-induced bacteriolysis (Fig. 4.4). Full length TcdE didn't induce lysis as shown by growth profiles and absent ATP release. Thus, it can be postulated that the hydrophilic, weak positively charged N-terminus (Fig. 5.2, green bar) prevents the first TMD from inserting into the cytoplasmic membrane resulting in insertion of only two TMDs (Fig. 5.2 [A], right panel) which probably are not capable of inducing lysis.
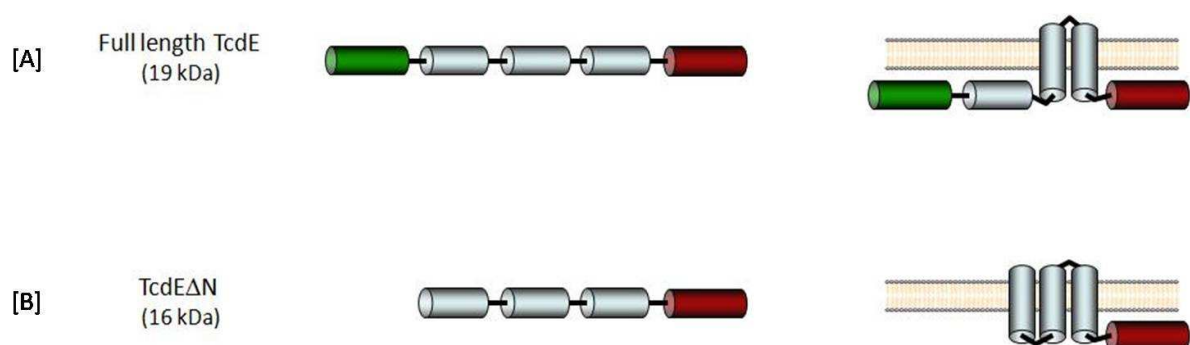
Fig. 5.2: Topological models for full length and truncated TcdE. [A] The 19 kDa full length TcdE possesses a hydrophilic, weakly positively charged N-terminus (green bar), three hydrophobic transmembrane domains (TMDs, grey bars) and a hydrophilic C-terminus (red bar). The N-terminus is supposed to retain the first TMD within the cytoplasm enabling insertion of only two TMDs into the cytoplasmic membrane (right panel). [B] The lack of the N-terminal region of TcdE allows the first TMD to insert into the membrane (right panel) leading to a potent lysis effector.

In contrast, truncated TcdE, consistent with the mutant TcdEΔN, lacks the N-terminal region and consequently enables the first transmembrane domain to insert into the membrane causing lysis of bacteria (Fig. 5.2 [B], right panel). This model is supported by the observation that the N-terminal deletion mutant TcdEΔN induced faster counterregulation of bacteria (Fig. 4.4 [A], blue curve) than wildtype TcdE expressing at least 5-10 % full length protein (Fig. 4.4 [A], red curve). The C-terminus probably has modulatory function and stabilizes the transmembrane domains within the cytoplasmic membrane.

The λ-holin derived protein products S105 and S107 only differ in a two amino acid extension of the antiholin S107 whereas the putative lytic TcdE (16 kDa truncated form) lacks about 25 amino acids compared to the putative inhibitor (19 kDa full length TcdE). Our data support the notion that lysis mechanism sensitively depended on N-terminal amino acid extensions of the truncated TcdE: an N-terminal located, weakly positively charged 6xHis-tag abolishes the bacteriolytic effect of TcdEΔN (not shown).

Taken together, the *tcdE* gene of *Clostridium difficile* exhibits a dual start motif resulting in the synthesis of two polypeptides, a 19 kDa full length and a 16 kDa truncated TcdE, the latter lacking the N-terminus only consisting of the three transmembrane domains (TMDs) and the C-terminus. *C. difficile* TcdE causes bacteriolysis of *E. coli* which is mediated by its truncated product, the N-terminal deleted 16 kDa protein. Alterations of the usually observed 1 : 10 ratio of full length to truncated TcdE with respect to higher quantities of the 19 kDa protein result in attenuation of the lytic properties indicating an inhibitory impact of the full length TcdE. It is suggested that lysis function requires oligomerization of TcdE monomers through their TMDs. The hydrophilic, weakly positively charged N-terminus of the full length TcdE presumably interacts with the inner surface of the cytoplasmic membranes preventing the first TMD from membrane insertion. In contrast, lack of the N-terminal region of the truncated TcdE enables all three TMDs to insert correctly into the cytoplasmic membranes and to form a lethal hole. A heterodimer of full length and truncated TcdE would be consequently less effective in lysis than a homodimer of N-terminal shortened TcdE.

5.2 *C. difficile* TcdE does not induce apoptosis

In addition to intestinal commensals, enterocytes are also in close vicinity to *Clostridium difficile.* Therefore, the enterocytes are possible targets for the holin-like TcdE, although eukaryotic cells differ fundamentally from prokaryotic cells in terms of their cellular structure, organization, metabolism and membrane composition (Tannert *et al.*, 2003). Recently it was shown by cell viability assays that the bacteriophage λ-holin is cytotoxic to eukaryotic cells accounting for a reduced tumor growth in vivo (Agu *et al.*, 2006). To

investigate the impact of *C. difficile* TcdE on eukaryotic cells, the capability of wildtype TcdE and/or the N-terminal deletion mutant TcdEΔN of releasing cytochrome *c* from isolated mitochondria was checked. Neither the mixture (ratio 1 : 10) of full length and truncated TcdE nor truncated TcdE alone caused mitochondria disruption. A putative impact of TcdE on the intact cell was studied by transfection of cells with the TcdE constructs to analyze cell and nuclei morphology and to detect putative activation of an apoptotic signal cascade.

Full length TcdE as well as the N-terminal shortened bacteriolytically active product was localized to the cytoplasm with a strong enrichment around the nucleus. Interestingly, TcdE didn't locate to cytoplasmic membranes as it was shown for prokaryotes. Similar observations were made with bacteriophage-encoded λ-holin. The presence of λ-holin protein in nuclei and cytoplasmic membranes was excluded. Instead, colocalization experiments confirmed localization of the holin in endomembranes, more precisely in the membranes of the endoplasmic reticulum (ER) and the mitochondria. This might be due to the bacterial ancestry of eukaryotic endomembranes (Agu *et al.*, 2007). The observed expression pattern of TcdE might also indicate localization of the hydrophobic TcdE within the eukaryotic endomembranes. The observed "maze-like" structures might represent the ER membranes within the cytoplasm with higher density around the nucleus. Additionally, the described bright "spots" can either be a result of accumulated protein due to high concentrations or might indicate localization of TcdE within the mitochondrial membranes. However, localization of a pore-forming protein within the ER membrane would have affected ER calcium homeostasis leading to cell death, as shown for aerolysin secreted by *Aeromonas hydrophila* (Krause *et al.*, 1998). The same would result upon pore-formation in the mitochondria membrane since membrane depolarization as consequence of non-selective diffusion of molecules across the mitochondrial inner membrane in turn leads to rapid ATP depletion and cell death (Kim *et al.*, 2003). Dependent on the mode of action apoptosis or oncosis occurs (Cherla *et al.*, 2003; Chakrabarti and McClane, 2005; Nottrott *et al.*, 2007). Apoptosis typically involves cellular shrinkage, nuclear condensation and fragmentation and the activation of caspases. However, neither expression of full length TcdE nor of the bacteriolytic short product altered morphology of nuclei up to 48 h after transfection or cell morphology, as shown on the basis of actin cytoskeleton staining. In addition, counterstain of the activated caspase-3 was performed but didn't provide an indication of TcdE inducing apoptosis. In reverse conclusion, a virulent impact of TcdE is most unlike.

5.3 TcdE in context of *Clostridium difficile* characteristics

5.3.1 Release of the toxins A and B

The previous results definitely excluded the notion of *Clostridium difficile* TcdE acting as pathogenicity factor. Instead, TcdE was investigated to obtain regulatory function with regard to release of the pathogenic toxins A and B. As shown, TcdE possesses a holin-like mode of action in bacteria as it induced lysis of *E. coli*. Since the toxins A and B lack signal peptides for extracellular secretion and no export mechanisms for the toxins are identified, TcdE was supposed to facilitate the release of the pathogenic glucosyltransferases from *C. difficile* to the extracellular environment (Tan *et al.*, 2001). This hypothesis was supported by the observation that *tcdE* was polycistronically transcribed together with the *tcdA-D* genes during the stationary phase of growth (Hundsberger *et al.*, 1997). Analysis of toxin production of the reference strain *C. difficile* VPI10463 confirmed an association between appearance of TcdE in the membrane fraction and accumulation of TcdA and TcdB in the respective supernatants (Fig. 4.12). To investigate a potential causal correlation between TcdE expression and toxin A/B release a TcdE deficient mutant was generated by insertional inactivation of the *tcdE* gene within *C. difficile* strain 630Δ*erm* (Chapters 4.4.1 and 4.4.2). This method is based on specific insertion of a modified group II intron into the target gene causing gene disruption and subsequent prevention of protein expression, as confirmed by Western blot analysis (Fig. 4.19). Comparative analysis of the *C. difficile* strain cdi630Δ*erm* and the respective TcdE- knockout strain cdi630Δ*tcdE* revealed almost equal toxin levels released into the supernatant. The data were confirmed by treatment of epithelial cells with the respective supernatants and a subsequent monitoring of the cytopathic effect (Fig. 4.21). Cytotoxicity induced by the toxins of the supernatants was comparable for both strains reflecting comparable toxin quantities. Hence, the release of the toxins is independent of TcdE. This outcome is corroborated by the observation that exclusively the full length TcdE (19 kDa) is produced in *C. difficile* whereas bacteriolysis in *E. coli* was induced by the 16 kDa, N-terminal shortened protein.

Moreover, the hypothesis that TcdE forms a lytic pore in *C. difficile* was questionable since the cytoplasmic membrane of Gram positive bacteria is covered by a thick, multilayered peptidoglycan requiring enzymes possessing murein hydrolase activity for its degradation. Although muralytic enzymes are known to be involved in completion of cell division of Gram positive bacteria (e.g. autolysin from *Staphylococcus aureus*) (Baba and Schneewind, 1998) and *C. difficile* phage φC2 was shown to exhibit a lysis module with holin and endolysin (Goh *et al.*, 2007), there was no indication of bacteriolysis of *C. difficile*. Additionally, analysis of the extracellular fraction of *C. difficile* VPI10463 revealed marginal amounts of cytoplasmic proteins reflecting a small fraction of lysed cells further arguing against bacterial lysis as route for release of the toxins A and B (Mukherjee *et al.*, 2002)

For these reasons *C. difficile* TcdE is excluded to participate in, much less, to be responsible for the release of the pathogenic toxins into the extracellular environment.

5.3.2 *C. difficile* growth and sporulation

The 16 kDa, N-terminal shortened TcdE was shown to be crucial for bacteriolysis in *E. coli* whereas the 19 kDa product had inhibitory effect concerning holin action and bacterial growth. Since *C. difficile* exclusively expresses the 19 kDa, full length protein (Fig. 4.12 (A) and Fig. 4.19) we addressed the question whether TcdE might also arrest growth of *C. difficile* and conceivably cause a shift to toxin synthesis. However, as shown in the former chapter TcdE did not affect the toxin levels released from *C. difficile*. Additionally, comparative analysis of time-dependent cell count of the *C. difficile* strain cdi630Δ*erm* and the TcdE deficient strain cdi630Δ*tcdE* demonstrated that TcdE is not involved in regulation of *C. difficile* growth as the resulting growth curves developed congruently (Fig. 4.22, filled squares).

The reference strain *C. difficile* VPI10463 and the hypervirulent strain 196 revealed conspicuous differences in sporulation efficacies (Fig. 4.15) as also observed with another PCR ribotype 027 strain by Akerlund and colleagues (Akerlund *et al*., 2008). Comparative analysis of TcdE expression of cdiVPI10463 and cdi196 was performed to examine a potential impact of TcdE in sporogenesis. TcdE production of both strains acted on the same kinetic but, interestingly, the high sporulating strain *C. difficile* 196 reflected an expression level which was 5-fold less than that of the low sporulating, high toxin producing strain VPI10463. Comparison of sporulation rates of cdi630Δ*erm* and the TcdE-knockout strain cdi630Δ*tcdE*, however, didn't verify a correlation (Fig. 4.22, filled circles). Indeed, cdi630Δ*tcdE* tended to exhibit a marginal higher sporulation rate after 48 h cultivation. But nevertheless, involvement of TcdE in sporogenesis can be excluded.

Apart from that, toxin release was accompanied by a reduction in cell count (Fig. 4.13) indicating a lysis- or sporulation- based release of TcdA and TcdB. Interestingly, the sporulation rate of the reference strain VPI10463 was only 5 % clearly arguing against a sporulation-mediated toxin release. Ketley and co-workers didn't show any correlation between TcdA release and sporogenesis in *C. difficile* strain 8089 either (Ketley *et al*., 1986). This result was confirmed by Mukherjee and colleagues since they found small amounts of typical cytoplasmic proteins in the culture supernatant of *C. difficile* strain VPI10463 probably reflecting small quantities of lysed respectively sporulated cells that cannot explain the efficient toxin release of 50 % (Mukherjee *et al*., 2002). In contrast, other previous studies showed a correlation of sporogenesis and toxin release (Boriello and Barclay, 1986; Kamiya *et al*., 1992) confirming the results obtained in this study concerning *C. difficile* strain 630Δ*erm* and the hypervirulent strain 196 showing that sporulation was accompanied by an increase of toxin levels in the supernatant.

Finally, data of this study evidenced that *C. difficile* TcdE is neither decisively involved in the release of the toxins into the extracellular environment nor in the regulation of bacterial growth and sporogenesis. The controversial results regarding the correlation of toxin release and sporulation obtained from the literature and from this study eventually excluded sporogenesis-mediated lysis as the route for the release of the toxins. The investigated strains indeed differed in sporulation frequency but were together comparable to release rate of their toxins.

5.4 Potential function of *C. difficile* TcdE

The small hydrophobic TcdE from *C. difficile* was examined with regard to a potential virulent impact on epithelial cells as intestinal targets. However, recombinant TcdE neither affected nuclei and cell morphology nor induced apoptotic signal cascades reflecting a non-pathogenic role in *C. difficile* associated disease. TcdE was furthermore excluded to participate in the release of the pathogenic toxins A and B or to influence *C. difficile* growth and be involved in sporogenesis.

TcdE induced bacteriolysis in *E. coli* mediated by an N-terminal shortened TcdE which expression is regulated by a dual start motif, as it is known for bacteriophage-encoded holins. From this observation a potential role of TcdE in *C. difficile* colonization could be construed since TcdE is simultaneously expressed with TcdA and TcdB. Lysis of the intestinal Gram negative commensals by TcdE would facilitate and advantage *C. difficile* colonization. A role as colonization factor has to be investigated in more detail in further studies.

Interestingly, previous studies identified homologies of *tcdE*, *tcdA* and *tcdC* to phage sequences of other species indicating that the pathogenicity locus of *C. difficile* was carried as part of a prophage that integrated at a specific site and conferred toxigenicity to ancestral *C. difficile* strains (Goh *et al.*, 2005a; Goh *et al.*, 2005b). *TcdE* was shown to be present in three temperate phages isolated from *C. difficile* (Goh *et al.*, 2005b) further arguing for a holin-like mode of action of TcdE. However, the lytic impact was not observed in *C. difficile*. This matches with previous studies that examined the composition of extracellular proteins of *C. difficile* and excluded bacterial lysis as the route of toxin release (Mukherjee *et al.*, 2002).

Since no contribution to growth regulation, sporogenesis and toxin release was observed for TcdE, the question arises about other tasks or whether TcdE has indirect functions. A hypothetical role might be to function as control element to prevent utilization of the pathogenicity locus through other bacterial species. In the case of phage infection, other bacteria species could gain access of the *C. difficile* PaLoc for instance through phage carriage or conjugation. The subsequent transcription under control of the alternative

ribosome binding sequence (Shine Dalgarno sequence) of *tcdE* would lead to an excess of truncated TcdE resulting - in cooperation with phage encoded endolysins - in lysis of the respective bacterium. Hence, *tcdE* could function like a Trojan Horse to defend the pathogenicity locus that is crucial for virulence of *C. difficile*.

Alternatively, in contrast to the hypothesized bacteriolytic impact, TcdE might defend *C. difficile* from phage-mediated lysis after infection. *C. difficile* phages are shown to exhibit a lysis module consisting of holin and endolysin genes, whose expression presumably would result in cell death of clostridia (Goh *et al.*, 2007). Since *C. difficile* exclusively produces full length TcdE, which acts as antiholin, TcdE could have antagonistic function towards the phage-holin and could cause deceleration or even inhibition of phage-induced lysis. Thus, this hypothesis would assign an indirect role in *C. difficile* colonization to TcdE as it potentially prolongs *C. difficile* survival after phage infection.

6. Bibliography

Agu CA, Klein R, Schwab S, König-Schuster M, Kodajova P, Ausserlechner M, Binishofer B, Bläsi U, Salmons B, Günzburg WH, Hohenadl C (2006). The cytotoxic activity of the bacteriophage λ-holin protein reduces tumour growth rates in mammary cancer cell xenograft models. *J Gene Med* 8: 229–241.

Agu CA, Klein R, Lengler J, Schilcher F, Gregor W, Peterbauer T, Bläsi U, Salmons B, Günzburg WH, Hohenadl C (2007). Bacteriophage-encoded toxins: the λ-holin protein causes caspase-independent non-apoptotic cell death of eukaryotic cells. *Cellular Microbiol* 9(7): 1753-1765.

Akerlund T, Persson I, Unemo M, Noren T, Svenungsson B, Wullt M, Burman LG (2008). Increased sporulation rate of epidemic Clostridium difficile Type 027/NAP1. *Journal of Clinical Microbiology* 46: 1530-1533.

Al-Nassir WN, Sethi AK, Nerandzic MM, Bobulsky GS, Jump RL, Donskey CJ (2008). Comparison of clinical and microbiological response to treatment of *Clostridium difficile*-associated disease with metronidazole and vancomycin. *Clin Infect Dis* 47: 56-62.

Aslam S, Hamill RJ, Musher DM (2005). Treatment of *Clostridium difficile*-associated disease: old therapies and new strategies. *Lancet Infect Dis.* 5: 549-557.

Baba T, Schneewind O (1998). Targeting of muralytic enzymes to the cell division site of Gram-positive bacteria: repeat domains direct autolysin to the equatorial surface ring of *Staphylococcus aureus*. *EMBO J* 17(16): 4639–4646.

Bartlett JG, Chang TW, Gurwith M, Gorbach SL, Onderdonk AB (1987). Antibiotic-associated pseudomembranous colitis due to toxin-producing clostridia. *N Engl J Med* 298:531-534.

Bartlett JG, Gerding DN (2008). Clinical recognition and diagnosis of Clostridium difficile infection. *Clin Infect Dis* 46 Suppl 1:S12-8.

Bläsi U, Nam K, Hartz D, Gold L, Young R (1989). Dual translational initiation sites control function of the lambda S gene. *EMBO J* 8(11): 3501-3510.

Bläsi U, Chang CY, Zagotta MT, Nam KB, Young R (1990). The lethal lambda S gene encodes its own inhibitor. *EMBO J* 9(4): 981-989.

Bläsi U, Young R (1996). Two beginnings for a single purpose: the dual start holins in the regulation of phage lysis. *Mol Microbiol* 21 (4): 675-682.

Bonovich MT, Young R (1991). Dual start motif in two lambdoid S genes unrelated to λ S. *J Bacteriol* 173: 2897-2905.

Borriello SP, Barclay FE (1986). An in-vitro model of colonisation resistance to *Clostridium difficile* infection. *JMed Microbiol* 21: 299-309.

Braun V, Hundsberger T, Luekel P, Sauerborn M, Von Eichel-Streiber C (1996). Definition of the single integration site of the pathogenicity locus in Clostridium difficile. *Gene* 181: 29-38.

Cartwright CP, Stock F, Beekmann SE, Williams EC, Gill VJ (1995)**.** PCR amplification of rRNA intergenic spacer regions as a method for epidemiologic typing of Clostridium difficile. *J Clin Microbiol* 33 (1): 1184-187.

Chang CY, Nam K, Young R (1995). S gene expression and the timing of lysis by bacteriophage λ. *J Bacteriol* 177: 3283–3294.

Chakrabarti G, McClane BA (2005). The importance of calcium influx, calpain and calmodulin for the activation of CaCo-2 cell death pathways by *Clostridium perfringens* enterotoxin. *Cell Microbiol* 7:129-146.

Cherla RP, Lee SY, Tesh VL (2003). Shiga toxins and apoptosis. *FEMS Microbiol Lett* 228: 159-166.

Dove CH, Wang SZ, Price SB, Phelps CJ, Lyerly DM, Wilkins TD, Johnson JL (1990). Molecular characterization of the *Clostridium difficile* toxin A gene. *Infect.Immun.* 58: 480-488.

Durai R. Epidemiology, pathogenesis, and management of *Clostridium difficile* infection (2007). *Dig Dis Sci*. 52(11):2958-62.

Frost F, Craun GF, Calderon RL (1998). Increasing hospitalization and death possibly due to Clostridium difficile diarrheal disease. *Emerging Infectious Diseases* 4: 619-625.

Gerding DN, Johnson S, Peterson LR, Mulligan ME, Silva J Jr (1995). *Clostridium difficile*-associated diarrhea and colitis. *Infect Control Hosp Epidemiol* 16(8):459-77.

Gerhard R, Nottrott S, Schoentaube J, Tatge H, Olling A, Just I (2008). Glucosylation of Rho GTPases by *Clostridium difficile* toxin A triggers apoptosis in intestinal epithelial cells. *J Med Microbiol* 57: 765-770.

Geric B, Carman RJ, Rupnik M, Genheimer CW, Sambol SP, Lyerly DM, Gerding DN, Johnson S (2006). Binary-toxin producing large clostridial toxin toxin-negative *Clostridium difficile* strains are enterotoxic but do not cause disease in hamsters. *J Infect Dis* 193: 1143-1150.

Goh S, Riley TV, Chang BJ (2005a). Isolation and characterization of temperate bacteriophages of Clostridium difficile. *Appl Environm Microbiol* 71(2): 1079-1083.

Goh S, Chang BJ, Riley TV (2005b). Effect of phage infection on toxin production by *Clostridium difficile*. *J Med Microbiol* 54: 129-135.

Goh S, Ong PF, Song KP, Riley T, Chang BJ (2007). The complete genome sequence of Clostridium difficile phage φC2 and comparisons to φCD119 and inducible prophages of CD630. *Microbiology* 153: 676-685.

Graschopf A, Bläsi U (1999). Molecular function of the dual start motif in the λ S holin. *Mol Microbiol.* 33: 569-582.

Gründling A, Smith DL, Bläsi U, Young R (2000). Dimerization between the holin and holin inhibitor of phage λ. *J Bacteriol* 182: 6075-6081.

Gründling A, Manson MD, Young R (2001). Holins kill without warning. *Proc.Natl.Acad.Sci* 98: 9348-9352.

Hall A (1998). Rho GTPases and the actin cytoskeleton. *Science* 279: 509-514.

Hall JC, O'Toole E (1935). Intestinal flora in new-born infants with a description of a new pathogenic anaerobe, *Bacillus difficilis*. *American Journal of Diseases of Children* 49: 390-402.

Hammond GA, Johnson JL (1995). The toxinogenic element of Clostridium difficile strain VPI 10463. *Microb.Pathogen* 19: 203-213.

Hammond GA, Lyerly DM, Johnson JL (1997). Transcritpional analysis of the toxigenic element of Clostridium difficile. *Microb Pathog* 22: 143-154

Heap JT, Pennington OJ, Cartman ST, Carter GP, Minton NP (2007). The ClosTron. A universal gene knockout system for the genus Clostridium. *J Microbiol Meth* 70: 452-464.

Hedge DD, Strain JD, Heins JR, Farver DK (2008). New advances in the treatment of *Clostridium difficile* infection (CDI). *Ther Clin Risk Manag* 4(5):949-64.

Hundsberger T, Braun V, Weidmann M, Leukel P, Sauerborn M, Von Eichel-Streiber C (1997). Transcription analysis of the genes *tcdA-E* of the pathogenicity locus of *Clostridium difficile. Eur J Biochem* 244: 735-742.

Hussain HA, Roberts AP, Mullany P (2005). Generation of an erythromycin-sensitive derivative of *Clostridium difficile* strain 630 (630Δ*erm*) and demonstration that the conjugative transposon Tn*916*ΔE enters the genome of this strain at multiple sites. *J Med Microbiol* 54: 137-141.

Jaffe AB, Hall A (2005). Rho GTPases: biochemistry and biology. *Annu Rev Cell Dev Biol* 21: 247-269.

Just I, Selzer J, Wilm M, Von Eichel-Streiber C, Mann M, Aktories K (1995a). Glucosylation of Rho proteins by *Clostridium difficile* toxin B. *Nature* 375: 500-503.

Just I, Wilm M, Selzer J, Rex G, Von Eichel-Streiber C, Mann M, Aktories K (1995b). The enterotoxin from *Clostridium difficile* (ToxA) monoglucosylates the Rho proteins. *J Biol Chem* 270: 13932-13936.

Just, I., Hofmann, F., Genth, H. Strategies against bacterial toxins in the gut: the case of *Clostridium difficile*. In: J.P. Galmiche (ed.) Novel Approaches in the treatment of gastointestinal and liver disease: a look in the future. John Libbey Eurotext **2000**, Montrouge, London, Rome, 33-35.

Karberg M, Guo H, Zhong J, Coon R, Perutka J, Lambowitz AM (2001). Group II introns as controllable gene targeting vectors for genetic manipulation of bacteria. *Nat Biotechnol* 19: 1162-1167.

Karlsson S, Dupuy B, Mukherjee K, Norin E, Burman LG, Akerlund T (2003). Expression of *Clostridium difficile* toxins A and B and their sigma factor TcdD is controlled by temperature. *Infect Immun* 71(4): 1784-93.

Ketley JM, Mitchell TJ, Haslam SC, Stephen J, Candy DCA, Burdon DW (1986). Sporogenesis and toxin A production by *Clostridium difficile*. *J Med Microbiol* 22: 33-38.

Kim JS, He L, Lemasters JJ (2003). Mitochondrial permeability transition: a common pathway to necrosis and apoptosis. *Biochem Biophys Res Commun* 304: 463-470.

Krause KH, Fivaz M, Monod A, van der Goot FG (1998). Aerolysin induces G-protein activation and Ca2+ release from intracellular stores in human granulocytes. *J Biol Chem* 273: 18122-18129.

Krupovic M, Bamford DH (2008). Holin of bacteriophage lambda: structural insights into membrane lesion. *Mol Microbiol* 69 (4): 781-783.

Larson HE, Proce AB (1977). Pseudomembranous colitis; presence of clostridial toxin. *Lancet* 2(8052-8053): 1312-1314.

Lawrence JP, Brevetti L, Obiso RJ, Wilkins TD, Kimura K, Soper R (1997). Effects of epidermal growth factor and Clostridium difficile toxin B in a model of mucosal injury. *J Pediatr Surg* 32(3): 430-433.

Leung D, Kelly CP, Boguniewicz M, Pothulakis C, LaMont JC, Flores A (1991). Treatment with intravenously administered gamma globulin of chronic relapsing colitis induced by Clostridium difficile toxin. *J Pediatr* 118 (4): 633-637.

Lillie RD (1977). The gram stain. A quick method for staining gram positive organisms in tissue. *Arch Path* 5: 828-834.

Lyerly DM, Lockwood DE, Richardson SH, Wilkins TD (1982). Biological activities of toxins A and B of *Clostridium difficile*. *Infect.Immun* 35: 1147-1150.

Lyerly DM, Saum KE, MacDonald DK, Wilkins TD (1985). Effects of *Clostridium difficile* toxins given intragastrically to animals. *Infect.Immun* 47: 349-352.

Lyerly DM, Wilkins TD (1995). *Clostridium difficile*. In: Blaser MJ, Smith PD, Ravdin JI, Greenberg HB, Guerrant RL, eds. *Infections of the Gastrointestinal Tract.* New York: Raven Press,Ltd., 867-891.

Lyras D, O'Connor JR, Howarth PM, Sambol SP, Carter GP, Phumoonna T, Poon R, Adams V, Vedantam G, Johnson S, Gerding DN, Rood JI (2009). Toxin B is essential for virulence of *Clostridium difficile*. *Nature* 458(7242): 1176-1179.

Makarova O, Kamberov E, Margolis B (2000). Generation of deletion and point mutations with one primer in a single cloning step. *Biotechniques* 29(5):970-972.

Mani N, Dupuy B (2001). Regulation of toxin synthesis in *Clostridium difficile* by an alternative RNA polymerase sigma factor. *Proc Natl Acad Sci* 98: 5844–5849.

Mani N, Lyras D, Barroso L, Howarth P, Wilkins T, Rood JI, Sonenshine AL, Dupuy B (2002). Environmental response and autoregulation of *Clostridium difficile* TxeR, a sigma factor for toxin gene expression. *J Bacteriol* 184: 5971–5978.

Matamouros S, England P, Dupuy B (2007). *Clostridium difficile* toxin expression is inhibited by the novel regulator TcdC. *Mol.Microbiol.* 64: 1274-1288.

McDonald LC, Killgore GE, Thompson A, Owens RC, Jr., Kazakova SV, Sambol SP, Johnson S, Gerding DN (2005). An epidemic, toxin gene-variant strain of *Clostridium difficile*. *New England J.Med.* 353: 2433-2441.

McFarland LV (2006). Meta-analysis of probiotics for the prevention of antibiotic associated diarrhea and the treatment of *Clostridium difficile* disease. *Am J Gastroenterol* 101 (4): 812-822.

Missiakas D, Raina S (1998). The extra-cytoplasmic function sigma factors: role and regulation. *Mol Microbiol* 28:1059–1066.

Mukherjee, K, Karlsson, S, Burman, LG, Akerlund, T (2002). Proteins released during high toxin production in *Clostridium difficile*. *Microbiology* 148: 2245-2253.

Musher DM, Aslam S, Logan N, Nallacheru S, Bhaila I, Borchert F, Hamill RJ (2005). Relatively poor outcome after treatment of *Clostridium difficile* colitis with metronidazole. *Clin Infect Dis* 40: 1586-1590.

Nottrott S, Schoentaube J, Genth H, Just I, Gerhard R (2007). Clostridium difficile toxin A-induced apoptosis is p53-independent but depends on glucosylation of Rho GTPases. *Apoptosis.* 12: 1443-1453.

Nusrat A, Von Eichel-Streiber C, Turner JR, Verkade P, Madara JL, Parkos CA (2001). *Clostridium difficile* toxins disrupt epithelial barrier function by alteringmembrane microdomain localization of tight junction proteins. *Infect Immun* 69(3): 1329–1336.

Owens RC (2007). *Clostridium difficile* –associated disease: changing epidemiology and implications in management. *Drugs* 67: 487-502.

Park T, Struck DK, Deaton JF, Young R (2006). Topological dynamics of holins programmed bacterial lysis. *PNAS* 103 (52): 19713-19718.

Park T, Struck DK, Dankenbring CA, Young R (2007). The Pinholin of lambdoid phage 21: control of lysis by membrane depolarization. *J Bacteriol* 189 (24): 9135-9139.

Pepin J, Valiquette L, Alary ME, Villemure P, Pelletier A, Forget K, Pepin K, Chouinard D (2004). *Clostridium difficile*-associated diarrhea in a region of Quebec from 1991 to 2003: a changing pattern of disease severity. *CMAJ.* 171: 466-472.

Perelle S, Gibert M, bourlioux P, Corthier G, Popoff MR (1997). Production of a complete binary toxin (actin-specific ADP-ribosyltransferase) by *Clostridium difficile* CD196. *Infect Immun* 65: 1402-1407.

Perfettini JL, Gissot M, Souque P, Ojcius DM (2002). Modulation of apoptosis during infection with Chlamydia*. Methods Enzymol* 58, 334-344.

Perutka J, Wang W, Goerlitz D, Lambowitz AM (2004). Use of computer-designed group II introns to disrupt Escherichia coli DExH/D-box protein and DNA helicase genes. *J Mol Biol* 336: 421-439.

Pituch H, van Leeuwen W, Maquelin K, Wultańska D, Obuch-Woszczatyński P, Nurzyńska G, Kato H, Reijans M, Meisel-Mikołajczyk F, Łuczak M, van Belkum A (2007). Toxin Profiles and Resistances to Macrolides and Newer Fluoroquinolones as Epidemicity Determinants of Clinical Isolates of *Clostridium difficile* from Warsaw, Poland. *J Clin Microbiol* 45(5): 1607–1610.

Poxton IR, McCoubrey JM, Blair G (2001). The pathogenicity of *Clostridium difficile*. *Clin Microbiol Infect* 7:421-7.

Rafferty ME, Baltch AL, Smith RP, Bopp RH, Rheal C, Tenover FC, Killgore GE, Lyerly DM, Wilkins TD, Schoonmaker DJ, Hannett GE, Shayegani M (1998). Comparison of Restriction Enzyme Analysis, Arbitrarily Primed PCR and Protein Profile Analysis Typing for Epidemiologic Investigation of an Ongoing *Clostridium difficile* Outbreak. *J Clin Microbiol* 36 (10): 2957-2963.

Riegler M, Sedivy R, Sogukoglu T, Castagliuolo I, Pothoulakis C, Cosentini E, Bischof G, Hamilton G, Teleky B, Feil W, Lamont JT, Wenzl E (1997). Epidermal growth factor attenuates Clostridium difficile toxin A- and B-induced damage of human colonic mucosa. *Am J Physiol* 273(5 Pt 1):G1014-22

Rubin MS, Bodenstein LE, Kent KC (1995). Severe *Clostridium difficile* colitis. *Dis Colon Rectum* 38: 350-354.

Rupnik M (2008). Heterogeneity of large clostridial toxins: importance of Clostridium difficile toxinotypes. *FEMS Microbiol Rev* 32: 541-555.

Rupnik M, Avesani V, Janc M, Von Eichel-Streiber C, Delmée M (1998). A novel toxinotyping scheme and correlation of toxinotypes with serogroups of *Clostridium difficile* isolates. *J Clin Microbiol* 36: 2240-2247.

Rupnik M, Grabnar M, Geric B (2003). Binary toxin producing Clostridium difficile strains. *Anaerobe* 9: 289-294.

Ryan GL, Rutenberg AD (2007). Clocking out: Phage-induced lysis of *Escherichia coli*. *J Bacteriol* 189 (13): 4749-4755.

Salcedo J, Keates S, Pothoulakis C, Warny M, Castagliuolo I, LaMont JT, Kelly CP (1997). Intravenous immunoglobulin therapy for severe *Clostridium difficile* colitis. *Gut* 41: 366-370.

Savva CG, Dewey JS, Deaton J, White RL, Struck DK, Holzenburg A, Young R (2008). The holin of bacteriophage lambda forms rings with large diameter. *Mol Microbiol* 69 (4): 784-793.

Sebaihia M, Wren BW, Mullany P, Fairweather NF, Minton N, Stabler R, Thomson NR, Roberts AP, Cerdeno-Tarraga AM, Wang H, Holden MT, Wright A, Churcher C, Quail MA, Baker S, Bason N, Brooks K, Chillingworth T, Cronin A, Davis P, Dowd L, Fraser A, Feltwell T, Hance Z, Holroyd S, Jagels K, Moule S, Mungall K, Price C, Rabbinowitsch E, Sharp S, Simmonds M, Stevens K, Unwin L, Whithead S, Dupuy B, Dougan G, Barrell B, Parkhill J (2006). The multidrug-resistant human pathogen Clostridium difficile has a highly mobile, mosaic genome. *Nat.Genet.* 38: 779-786.

Seehase S (2008). Wirkung von *Clostridium difficile* TcdE auf die Proliferation von *Escherichia coli*. Diploma thesis in the Institute of Toxicology, Hannover Medical School.

Savva CG, Dewey JS, Deaton J, White RL, Struck DK, Holzenburg A, Young R (2008). The holin of bacteriophage lambda forms rings with large diameter. *Mol Microbiol* 69 (4): 784-793.

Schoentaube J, Olling A, Tatge H, Just I, Gerhard R (2009). Serine-71 phosphorylation of Rac1/Cdc42 diminishes the pathogenic effect of *Clostridium difficile* toxin A. *accepted*

Surowiec D, Kuyumjian AG, Wynd MA, Cicogna CE (2006). Past, present, and future therapies for *Clostridium difficile*-associated disease. *Ann Pharmacother.* 40: 2155-2163

Tan KS, Wee BY, Song KP (2001). Evidence for holin function of tcdE gene in the pathogenicity of *Clostridium difficile. J Med Microbiol* 50(7): 613-619.

Tannert A, Pohl A, Pomorski T, Herrmann A (2003). Protein-mediated transbilayer movement of lipids in eukaryotes and prokaryotes: the relevance of ABC transporters. *Int J Antimicrob Agents* 22: 177-187.

Triadafilopoulos G, Pothoulakis C, O'Brien MJ, LaMont JT (1987). Differential effects of *Clostridium difficile* toxins A and B on rabbit ileum. *Gastroenterology* 93: 273-279.

Von Eichel-Streiber C, Harperath U, Bosse D, Hadding U (1987). Purification of two high molecular weight toxins of Clostridium difficile which are antigenetically related. *Microb Pathogen* 2: 307-318.

Von Eichel-Streiber C, Sauerborn M (1990). Clostridium difficile toxin A carries a C-terminal repetetive structure homologous to the carbohydrate binding region of streptococcal glycosyltransferases. *Gene* 96: 107-113.

Von Eichel-Streiber C, Laufenberg-Feldmann R, Sartingen S, Schulze J, Sauerborn M (1992). Comparative sequence analysis of the Clostridium difficile toxins A and B. *Mol Gen Genet* 233: 260-268.

Wang IN, Smith DL, Young R (2000). Holins: the protein clocks of bacteriophage infections. *Annu Rev Microbiol* 54: 799-825.

Wang IN, Deaton J, Young R (2003). Sizing the holin lesion with an endolysin-beta-galactosidase fusion. *J Bacteriol* 185: 779-787.

Warny M, Pepin J, Fang A, Killgore G, Thompson A, Brazier J, Frost E, McDonald LC (2005). Toxin production by an emerging strain of Clostridium difficile associated with outbreaks of severe disease in North America and Europe. *Lancet* 366: 1079-1084.

Wenisch C, Parschalk B, Hasenhündl M, Hirschl AM, Graninger W (1996). Comparison of vancomycin, teicoplanin, metronidazole, and fusidic acid for the treatment of *Clostridium difficile-* associated diarrhea. *Clinical Infectious Diseases* 22: 813-818.

Wessel D, Flugge UI (1984). A method for the quantitative recovery of protein in dilute solution in the presence of detergents and lipids. *Anal Biochem* 138: 141-143.

Wolff D, Brüning T, Gerritzen A (2009). Rapid detection of the *Clostridium difficile* ribotype 027 *tcdC* gene frame shift mutation at position 117 by real-time PCR and melt curve analysis. *Eur J Clin Microbiol Infect Dis* [Epub ahead of print].

Young R (1992). Bacteriophage lysis: mechanism and regulation. *Microbiol Rev* 56: 430-481.

Young R, Bläsi U (1995). Holins: form and function in bacteriophage lysis. *FEMS Microbiol Rev* 17: 191-205.

Young R, Wang I-N, Roof WD (2000). Phages will out: strategies of host cell lysis. *Trends Microbiol* 8 (3): 120-128.

Zar FA, Bakkanagari SR, Moorthi KM, Davis MB (2007). A comparison of vancomycin and metronidazole for the treatment of *Clostridium difficile*-associated diarrhea, stratified by disease severity. *Clin Infect Dis* 45: 302-307.

7. List of Abbreviations

AEBSF	4-(2-Aminoethyl) benzenesulfonyl fluoride hydrochloride
ATP	adenosine 5'-triphosphate
BSA	bovine serum albumin
CDAD	Clostridium difficile-associated diarrhea
DAPI	4',6'-diamidino-2-phenylindole hydrochloride
DNA	desoxy ribonucleic acid
dNTPs	deoxynucleotide-triphosphates
DTT	dithiothreitol
EDTA	ethylene diamine tetraacetic acid
ELISA	enzyme-linked immunosorbent assay
FBS	fetal bovine serum
HCL	hydrochloride acid
Hepes	4-(2-hydroxyethyl)-1-piperazineethanesulfonic acid
IPTG	isopropyl-D-thiogalatopyranosid
LB	Luria Bertani
MEM	Minimum Essential Medium
MgCl$_2$	magnesium chloride
OD$_{600}$	optical density at 600 nm
PAGE	polyacrylamid electrophoresis
PBS	phosphate buffered saline
PCR	polymerase chain reaction
SDS	sodium dodecyl sulfate
SOE-PCR	Splicing by overlap extension PCR
S105	holin protein of lambda phage
S107	antiholin protein of lambda phage
TBST	Tris buffered saline Tween-20
TcdA	*Clostridium difficile* toxin A
TcdB	*Clostridium difficile* toxin B
TcdC	*Clostridium difficile* toxin C
TcdD	*Clostridium difficile* toxin D
TcdE	*Clostridium difficile* toxin E
TMD	transmembrane domain
TNF-α	tumor necrosis factor α
Tris	tris(hydroxymethyl)-aminomethan
U	unit

A. Supplements

A.1 Nucleotide sequences of generated pQE30 constructs

The multiple cloning site of vector pQE30 contains the following inserted TcdE fragments. The ATG start codons are highlighted in green and the recognition sites of the respective endonucleases in blue: BamHI (5' end) and Hind III (3' end). Bases encoding the 6xHistidine tag are underlined. This region is deleted in constructs pQE30-TcdEΔN and pQE30-TcdEΔNΔC. The alternative Shine-Dalgarno sequence is underlined in red and mutations are highlighted in red.

Full length TcdE (*C. difficile* strain VPI10463)

```
ATGAGAGGATCGCATCACCATCACCATCACGGATCCATGCACAGTAGTTCACCTTTTTA
TATTTCTAATGGTAACAAAATATTTTTTTATATAAACCTAGGAGGCGTTATGAATATGA
CAATATCTTTTTTATCAGAGCATATATTTATAAAGTTAGTAATTTTAACTATATCATTT
GATACATTATTAGGATGTTTAAGTGCAATAAAAAGTCGTAAATTTAATTCTAGTTTTGG
AATAGATGGAGGAATCAGAAAAGTAGCAATGATAGCATGTATATTTTTTTTATCAGTAG
TTGACATTCTTACAAAGTTTAACTTTTTATTTATGTTACCACAAGATTGTATCAATTTT
TTAAGACTAAAACATCTTGGAATATCTGAATTTTTCTCTATTTTATTTATTTTATATGA
AAGTGTAAGTATATTAAAAAATATGTGCTTATGTGGATTACCAGTACCTAAGAGATTAA
AGGAAAAAATAGCAATTTTACTAGATGCAATGACAGATGAAATGAATGCTAAGGGTGAA
AAGAAGCTT
```

TcdE-NC (N-terminus: *C. difficile* strain 8864; C-terminus: *C. difficile* strain VPI10463)

```
ATGAGAGGATCGCATCACCATCACCATCACGGATCAATGCACAGTAGTTCACCTTTATA
TTTTAATGGTAACAAAATATTTTTTTATATAAACCTAGGGGGCGTTATGAATATGGGTG
GTGGTGGTGGATCTAATATGTGCTTATGTGGATTACCAGTACCTAAGAGATTAAAGGAA
AAAATAGTAGTTTTACTAGATGCAATGACAGATGAAATGAATGCTAAGGGTGAAAAGGG
ATCCGGTGGTAAGCTT
```

TcdEΔN (*C. difficile* strain VPI10463)

```
ATGACAATATCTTTTTTATCAGAGCATATATTTATAAAGTTAGTAATTTTAACTATATC
ATTTGATACATTATTAGGATGTTTAAGTGCAATAAAAAGTCGTAAATTTAATTCTAGTT
TTGGAATAGATGGAGGAATCAGAAAAGTAGCAATGATAGCATGTATATTTTTTTTATCA
GTAGTTGACATTCTTACAAAGTTTAACTTTTTATTTATGTTACCACAAGATTGTATCAA
TTTTTTAAGACTAAAACATCTTGGAATATCTGAATTTTTCTCTATTTTATTTATTTTAT
ATGAAAGTGTAAGTATATTAAAAAATATGTGCTTATGTGGATTACCAGTACCTAAGAGA
```

```
TTAAAGGAAAAAATAGCAATTTTACTAGATGCAATGACAGATGAAATGAATGCTAAGGG
TGAAAAGAAGCTT
```

TcdEΔNΔC (*C. difficile* strain VPI10463)

```
ATGACAATATCTTTTTTATCAGAGCATATATTTATAAAGTTAGTAATTTTAACTATATC
ATTTGATACATTATTGGGATGTTTAAGTGCAATAAAAAGTCGTAAATTTAATTCTAGTT
TTGGAATAGATGGAGGAATCAGAAAAGTAGCAATGATAGCATGTATATTTTTTTTATCA
GTAGTTGACATTCTTACAAAGTTTAACTTTTTATTTATGTTACCACAAGATTGTATCAA
TTTTTTAAGACTAAAACATCTTGGAATATCTGAATTTTTCTCTATTTTATTTATTTTAT
ATGAAAGTGTAAGTATATTAAAAAATATGTAGAAGCTT
```

TcdE Shine-Dalgarno mutant I (TcdE SDI)

```
ATGAGAGGATCGCATCACCATCACCATCACGGATCCATGCACAGTAGTTCACCTTTTTA
TATTTCTAATGGTAACAAAATATTTTTTTATATAAACCTATTAGGCGTTATGAATATGA
CAATATCTTTTTTATCAGAGCATATATTTATAAAGTTAGTAATTTTAACTATATCATTT
GATACATTATTAGGATGTTTAAGTGCAATAAAAAGTCGTAAATTTAATTCTAGTTTTGG
AATAGATGGAGGAATCAGAAAAGTAGCAATGATAGCATGTATATTTTTTTATCAGTAG
TTGACATTCTTACAAAGTTTAACTTTTTATTTATGTTACCACAAGATTGTATCAATTTT
TTAAGACTAAAACATCTTGGAATATCTGAATTTTTCTCTATTTTATTTATTTTATATGA
AAGTGTAAGTATATTAAAAAATATGTGCTTATGTGGATTACCAGTACCTAAGAGATTAA
AGGAAAAAATAGCAATTTTACTAGATGCAATGACAGATGAAATGAATGCTAAGGGTGAA
AAGAAGCTT
```

TcdE Shine-Dalgarno mutant II (TcdE SD II)

```
ATGAGAGGATCGCATCACCATCACCATCACGGATCCATGCACAGTAGTTCACCTTTTTA
TATTTCTAATGGTAACAAAATATTTTTTTATATAAACCTATTAGTCGTTATGAATATGA
CAATATCTTTTTTATCAGAGCATATATTTATAAAGTTAGTAATTTTAACTATATCATTT
GATACATTATTAGGATGTTTAAGTGCAATAAAAAGTCGTAAATTTAATTCTAGTTTTGG
AATAGATGGAGGAATCAGAAAAGTAGCAATGATAGCATGTATATTTTTTTATCAGTAG
TTGACATTCTTACAAAGTTTAACTTTTTATTTATGTTACCACAAGATTGTATCAATTTT
TTAAGACTAAAACATCTTGGAATATCTGAATTTTTCTCTATTTTATTTATTTTATATGA
AAGTGTAAGTATATTAAAAAATATGTGCTTATGTGGATTACCAGTACCTAAGAGATTAA
AGGAAAAAATAGCAATTTTACTAGATGCAATGACAGATGAAATGAATGCTAAGGGTGAA
AAGAAGCTT
```

TcdE Methionine mutant II (TcdE Met)

```
ATGAGAGGATCGCATCACCATCACCATCACGGATCCATGCACAGTAGTTCACCTTTTTA
TATTTCTAATGGTAACAAAATATTTTTTTATATAAACCTAGGAGGCGTTGCGAATTGCA
CAATATCTTTTTTATCAGAGCATATATTTATAAAGTTAGTAATTTTAACTATATCATTT
GATACATTATTAGGATGTTTAAGTGCAATAAAAAGTCGTAAATTTAATTCTAGTTTTGG
```

```
AATAGATGGAGGAATCAGAAAAGTAGCAATGATAGCATGTATATTTTTTTATCAGTAG
TTGACATTCTTACAAAGTTTAACTTTTTATTTATGTTACCACAAGATTGTATCAATTTT
TTAAGACTAAAACATCTTGGAATATCTGAATTTTTCTCTATTTTATTTATTTTATATGA
AAGTGTAAGTATATTAAAAAATATGTGCTTATGTGGATTACCAGTACCTAAGAGATTAA
AGGAAAAAATAGCATTTTACTAGATGCAATGACAGATGAAATGAATGCTAAGGGTGAA
AAG**AAGCTT**
```

A.2 Nucleotide sequences of generated pcDNA3.1 constructs

The multiple cloning site of vector pcDNA3.1(-)A contains the following inserted TcdE fragments. The ATG start codons are highlighted in green and the recognition sites of the respective endonucleases in blue: XhoI (5' end) and BamHI (3' end). Bases encoding the 6xHistidine tag are underlined. The myc epitope is highlighted by a dashed line.

Full length TcdE (*C. difficile* strain VPI10463)

```
**CTCGAG**CG**ATG**CACAGTAGTTCACCTTTTTATATTTCTAATGGTAACAAAATATTTTTT
TATATAAACCTAGGAGGCGTT**ATG**AAT**ATG**ACAATATCTTTTTTATCAGAGCATATATT
TATAAGTTAGTAATTTTAACTATATCATTTGATACATTATTAGGATGTTTAAGTGCAA
TAAAAAGTCGTAAATTTAATTCTAGTTTTGGAATAGATGGAGGAATCAGAAAAGTAGCA
ATGATAGCATGTATATTTTTTTATCAGTAGTTGACATTCTTACAAAGTTTAACTTTTT
ATTTATGTTACCACAAGATTGTATCAATTTTTTAAGACTAAAACATCTTGGAATATCTG
AATTTTTCTCTATTTTATTTATTTTATATGAAAGTGTAAGTATATTAAAAAATATGTGC
TTATGTGGATTACCAGTACCTAAGAGATTAAAGGAAAAAATAGCAATTTTACTAGATGC
AATGACAGATGAAATGAATGCTAAGGGTGAAAAG**GGATCC**GAGCTCGGTACCAAGCTTG
GGCCCGAACAAAAACTCATCTCAGAAGAGGATCTGAATAGCGCCGTCGACCATCATCAT
CATCATCATTGA
```

TcdEΔN (*C. difficile* strain VPI10463)

```
**CTCGAG**CG**ATG**ACAATATCTTTTTTATCAGAGCATATATTTATAAGTTAGTAATTTTA
ACTATATCATTTGATACATTATTAGGATGTTTAAGTGCAATAAAAAGTCGTAAATTTAA
TTCTAGTTTTGGAATAGATGGAGGAATCAGAAAAGTAGCAATGATAGCATGTATATTTT
TTTATCAGTAGTTGACATTCTTACAAAGTTTAACTTTTTATTTATGTTACCACAAGAT
TGTATCAATTTTTTAAGACTAAAACATCTTGGAATATCTGAATTTTTCTCTATTTTATT
TATTTTATATGAAAGTGTAAGTATATTAAAAAATATGTGCTTATGTGGATTACCAGTAC
CTAAGAGATTAAAGGAAAAAATAGCAATTTTACTAGATGCAATGACAGATGAAATGAAT
GCTAAGGGTGAAAAG**GGATCC**GAGCTCGGTACCAAGCTTGGGCCCGAACAAAAACTCAT
CTCAGAAGAGGATCTGAATAGCGCCGTCGACCATCATCATCATCATCATTGA
```

A.3 Expected Cdi630-tcdE-234a targeting region

The recognition sites of the respective endonucleases are highlighted in blue: HindIII (5' end) and BsrGI (3' end). The sequences of primers used for SOE-PCR are underlined: IBS (green), EBS2 (red) and EBS1d (blue).

```
AAAAAAGCTTATAATTATCCTTAAATATCCATGCTGTGCGCCCAGATAGGGTGTTAAGT
CAAGTAGTTTAAGGTACTACTCTGTAAGATAACACAGAAAACAGCCAACCTAACCGAAA
AGCGAAAGCTGATACGGGAACAGAGCACGGTTGGAAAGCGATGAGTTACCTAAAGACAA
TCGGGTACGACTGAGTCGCAATGTTAATCAGATATAAGGTATAAGTTGTGTTTACTGAA
CGCAAGTTTCTAATTTCGATTATATTTCGATAGAGGAAAGTGTCTGAAACCTCTAGTAC
AAAGAAAGGTAAGTTAATAGCATGGACTTATCTGTTATCACCACATTTGTACAATCTG
```

A.4 Plasmid map of pMTL007C-E2

SOE-PCR is used to alter the IBS, EBS2 and EBS1d sequences and the resulting fragment is cloned between the HindIII and BsrGI sites to re-target the plasmid. RAM-E2 reflects the Retrotransposition-activated selectable marker coding for an erythromycin resistance which is activated after successful integration of the modified intron into the right target site.
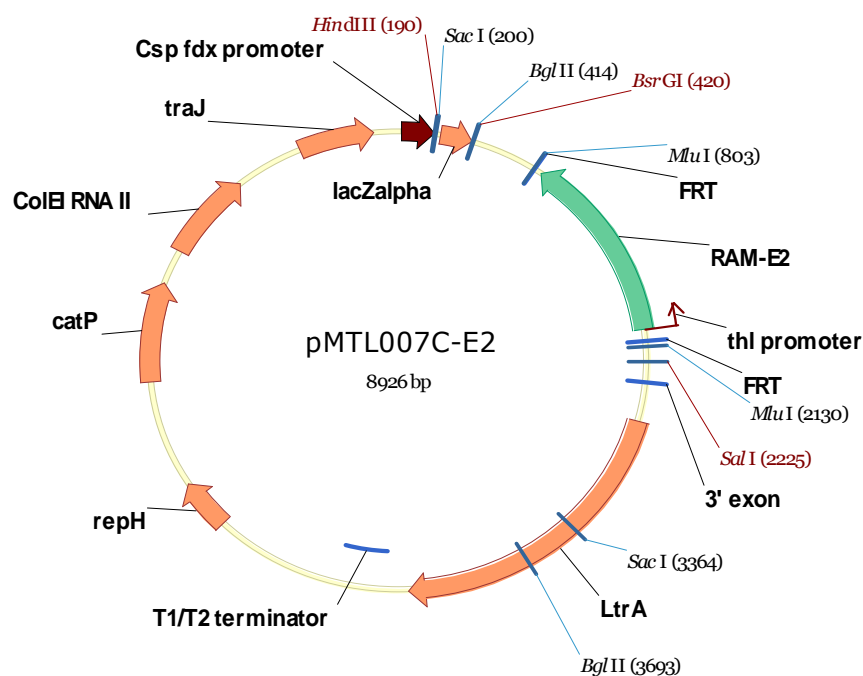
Plasmid pMTL007C-E2 was kindly provided by N. Minton (Centre for Biomolecular Sciences, University of Nottingham).

B. Curriculum Vitae

PERSONAL DATA

Name:	Alexandra Olling
Address:	Simrockstraße 27, 30171 Hannover
Phone:	+49 (0)511 8078891
E-Mail:	a_olling@yahoo.de
Date of Birth:	October 2nd 1980
Place of Birth:	Barßel, Germany
Nationality:	German

EDUCATION

07/2006 - 06/2009	Dissertation at the Institute of Toxicology, Hannover Medical School, supervised by PD Dr. Ralf Gerhard
02-06/2006	Graduate assistant at the Institute of Molecular and Cellular Physiology, Hannover Medical School
10/2000 – 11/2005	Study of Biochemistry, Gottfried Wilhelm Leibniz University, Hannover (Grade: "gut")
	Diploma thesis "Biochemical characterization of β-myosin from single fibers of human skeletal muscles with point mutations in the myosin head domain using flash photolysis of caged ATP compounds" at the Institute of Molecular and Cellular Physiology, Hannover Medical School, supervised by Prof. Dr. Theresia Kraft (Grade: "sehr gut")
07/2000	Abitur (Grade: 2.5)
08/1993 – 07/2000	Albertus-Magnus-Gymnasium, Friesoythe
08/1991 – 07/1993	"Orientierungsstufe" Schulzentrum Saterland, Ramsloh
08/1987 – 07/1991	Primary School, Strücklingen

Academic publications

Olling A, Seehase S, Tatge H, Schröter S, Minton N, Just I, Gerhard R. TcdE: Dual function in *E. coli* but no function in *C. difficile*? *Manuscript in preparation*

Schoentaube J, **Olling A**, Tatge H, Just I, Gerhard R (2009). Serine-71 phosphorylation of Rac1/Cdc42 diminishes the pathogenic effect of *Clostridium difficile toxin* A. *Cell Microbiol* [Epub ahead of print]

Kreimeyer I, Marckscheffel A, Tatge H, Pich A, **Olling A**, Schoentaube J, Just I, Gerhard R (2009). Autoproteolytic cleavage is not essential for the cytopathic effect of *Clostridium difficile* toxin A. *submitted to JBC*

Gerhard R, Nottrott S, Schoentaube J, Tatge H, **Olling A**, Just I (2008). Glucosylation of Rho GTPases by *Clostridium difficile* toxin A triggers apoptosis in intestinal epithelial cells. *J Med Microbiol* 57: 765-770.

Oral presentations

Villars-sur-Ollon (Switzerland), 5-9 October 2008. 4th Conference on New Frontiers in Microbiology and Infection. Clostridia: from Old Diseases to New Threats.
Olling A, Seehase S, Tatge H, Just I, Gerhard R (2008). Structure-function analysis of *Clostrdidium difficile* TcdE expressed in *Escherichia coli*. *Abstract Book P.14: 21*.

Poster presentations

Mainz (Germany), 11-13 March 2008. 49th Annual Meeting of the German Society of Pharmacology and Toxicology.
Olling A, Seehase S, Tatge H, Just I, Gerhard R (2008). The expression of *Clostridium difficile* TcdE affects bacterial growth. *Naunyn-Schmiedeberg's Archives of Pharmacology, 377:29, 112. Suppl. 1.*

Mainz (Germany), 10-12 March 2009. 50th Annual Meeting of the German Society of Pharmacology and Toxicology.
Olling A, Seehase S, Tatge H, Just I, Gerhard R (2009). Structure-function analysis of the holin-like TcdE from *Clostridium difficile. Naunyn-Schmiedeberg's Archives of Pharmacology, 379:25, 97. Suppl. 1.*

Torquay, Devon (United Kingdom), 1-4 December 2008. Marie Curie Conferences and Workshops on Clostridia. Event 9. Clostridium perfringens: The Conference.
Olling A, Seehase S, Tatge H, Just I, Gerhard R (2008). Structure-function analysis of the holin-like TcdE from *Clostridium difficile. Abstract Book*.

Languages

German   native language
English   fluent
French   basic